Paleobiology, 44(4), 2018, pp. 660–683
DOI: 10.1017/pab.2018.28

PALEOBIOLOGY
A PUBLICATION OF THE Paleontological SOCIETY

Taxonomic and evolutionary pattern revisions resulting from geometric morphometric analysis of Pennsylvanian *Neognathodus* conodonts, Illinois Basin

Alexander N. Zimmerman, Claudia C. Johnson, and P. David Polly

Abstract.—Conodont fossils are highly valuable for Paleozoic biostratigraphy and for interpreting evolutionary change, but identifying and describing conodont morphologies, and characterizing gradual shape variation remain challenging. We used geometric morphometric (GM) analysis to conduct the first landmark-based morphometric analysis of the biostratigraphically useful conodont genus *Neognathodus*. Our objective is to assess whether previously defined morphotype groups are reliably distinct from one another. As such, we reevaluate patterns of morphologic change in *Neognathodus* P1elements, perform maximum-likelihood tests of evolutionary modes, and construct novel, GM-based biozonations through a Desmoinesian (Middle Pennsylvanian) section in the Illinois Basin. Our GM results record the entire spectrum of shape variability among *Neognathodus* morphotypes, thus alleviating the problem of documenting and classifying gradual morphologic transitions between morphotypes. Statistically distinct GM groups support previously established classifications of *N. bassleri*, *N. bothrops*, and *N. roundyi*. Statistically indistinct pairs of GM groups do not support literature designations of *N. medadultimus* and *N. medexultimus*, and *N. dilatus* and *N. metanodosus*, and we synonymize each pair. Maximum-likelihood tests of evolutionary modes provide the first statistical assessment of *Neognathodus* evolutionary models in the Desmoinesian. The most likely evolutionary models are an unbiased random walk or a general random walk. We name four distinct biozones through the Desmoinesian using GM results, and these align with previous biozonation structure based on the *Neognathodus* Index (NI), illustrating that *Neognathodus*-based biostratigraphic correlations would not change between GM or NI methods. The structural similarity between both biozonations showcases that determining GM-based biozones is not redundant, as this comparison validates using landmark-based GM work to construct viable biozonations for subsequent stratigraphic correlations. Although this study is limited to the Illinois Basin, our quantitative methodology can be applied broadly to test taxonomic designations of additional genera, interpret statistically robust evolutionary patterns, and construct valid biozones for this significant chordate group.

Alexander N. Zimmerman, Claudia C. Johnson, and P. David Polly. 1001 East 10th Street, Department of Earth and Atmospheric Sciences, Indiana University, Bloomington, Indiana 47405-140 U.S.A.
E-mail: alexzimm@indiana.edu

Accepted: 14 July 2018
Published online: 30 August 2018
Data available from the Dryad Digital Repository: https://doi.org/10.5061/dryad.1fm52vv

Introduction

Characterizing morphologic variation within fossil groups is fundamental for determining taxonomic boundaries and interpreting evolution of extinct taxa (George 1956; Gingerich 1985), yet challenges remain in capturing the full range of shape variability within species (Allmon 2013). Paleontological species cannot rely on the biologic species concept (Mayr 1957, 1996) and thus are determined using the morphological species concept (George 1956; Gingerich 1985; Allmon 2013). Commonly, species are classified using qualitative and ultimately subjective morphologic metrics that may overemphasize the significance of shape difference or fail to capture the full range of form variation within a given species' population (Vogt et al. 2009; Allmon 2013). Temporal and spatial shape variability within a fossil group further complicates characterizing shape variation (Allmon 2013). Finding objective methods to record the spectrum of morphologic variation within extinct taxa is particularly valuable for biostratigraphically useful groups such as conodonts, because subjective morphologic criteria commonly lead to disagreements that affect stratigraphic correlations (Girard and Renaud 2011).

Since their discovery 160 years ago by Pander (1865), conodonts have become highly important biostratigraphic markers for Paleozoic strata (Donoghue et al. 1998; Sweet and

 0094-8373/18

Donoghue 2001), but debates persist surrounding conodont taxonomy (Aldridge and Purnell 1996; Barrick et al. 2004; Brown et al. 2016). Certain conodonts exhibited cosmopolitan distributions and evolving morphologies that provide an excellent record of morphologic change throughout the Paleozoic and Triassic (Sweet 1988; Sweet and Donoghue 2001) and an evolutionarily significant history of early chordate evolution (Purnell 1995; Aldridge and Purnell 1996; Donoghue et al. 1998; Donoghue et al. 2006). Nevertheless, disagreements regarding morphologic variation within and among species persist and fuel continual debate regarding evolutionary interpretations and biostratigraphic utility of certain conodont taxa (Barrick et al. 1996, 2004; Rexroad et al. 2001; Brown et al. 2016).

To help resolve these debates, conodont workers have employed quantitative methods to characterize certain conodont morphologies. Many researchers used Fourier analysis of outlines to test species groupings (Klapper and Foster 1986, 1993; Sloan 2003; Girard et al. 2004b, 2007). These studies validated the use of outline methods for characterizing conodont morphology and demonstrated that species boundaries are commonly gradational. Others demonstrated that patterns of morphologic change can be characterized quantitatively through time with outline methods (Murphy and Cebecioglu 1987; Renaud and Girard 1999; Girard et al. 2004a; Roopnarine et al. 2004; Jones and Purnell 2007). These results provide a useful foundation for the validity of conodont morphometric work, but all studies lacked a direct evaluation of how morphometric results would affect evolutionary interpretations and biozonations. We concur that assessing the influence of morphometric results on previous biozonations is highly valuable for such a biostratigraphically useful fossil group.

Here, we build on previous morphometric conodont work by conducting the first landmark-based geometric morphometric (GM) analysis (Bookstein 1991; Zelditch et al. 2004) of the biostratigraphically useful conodont genus *Neognathodus* and by evaluating how our results compare with evolutionary interpretations and previous biozonations. In addition, we conduct the first statistical assessment of *Neognathodus* evolutionary models in the Desmoinesian using methods developed by Hunt (2006) and used by many other researchers (Novack-Gottshall 2008; Jones 2009; Piras et al. 2012; Van Bocxlaer and Hunt 2013). GM analysis allows us to both quantify the continuous shape variation of P1 elements of *Neognathodus* morphotypes without placing specimens into different groups a priori and test whether established morphotype groups are reliably distinct from one another. Hunt's (2006) approach also allows us to minimize a priori assumptions, as the method does not assume a null hypothesis for any given evolutionary mode and does not favor any one evolutionary model a priori over others. Instead, it allows us to test all three modes simultaneously and compare each with equal weight based on the numeric data (Hunt 2006).

Evolution of *Neognathodus* species through time is particularly well documented, as the species are used to correlate Desmoinesian (Middle Pennsylvanian) strata in North America, most commonly in the Illinois Basin (Fig. 1); (Merrill 1972, 1975a,b; Grayson et al. 1985; Brown et al. 1991, 2013, 2016; Rexroad et al. 1998, 2001; Brown and Rexroad 2009). *Neognathodus* species are defined as populations of morphotypes, and morphotypes are classified by the morphology of the P1 (platform) element (Merrill 1972, 1975a,b, 1999). The species name corresponds to the predominant morphotype in the population (Merrill 1972, 1999). Interpretations of *Neognathodus* evolution and biozonation were summarized using the *Neognathodus* Index (NI), a weighted average of the morphotype population (i.e., the species) in a given stratigraphic unit (Brown et al. 2016). The NI relies on qualitative and subjective groupings of morphotypes (Brown and Rexroad 2009). Furthermore, Merrill (1972, 1975a,b, 1999) documented a gradational transition in shape between morphotype groups. Thus, classifying specimens into separate morphotype groups may not effectively capture the range of transitional shape variation.

Our study addresses three questions and their subsequent hypotheses. (1) Are the GM groups of *Neognathodus* congruent or incongruent with published morphotype groups of *N. bassleri* (Harris and Hollingsworth 1933);

https://doi.org/10.1017/pab.2018.28 Published online by Cambridge University Press

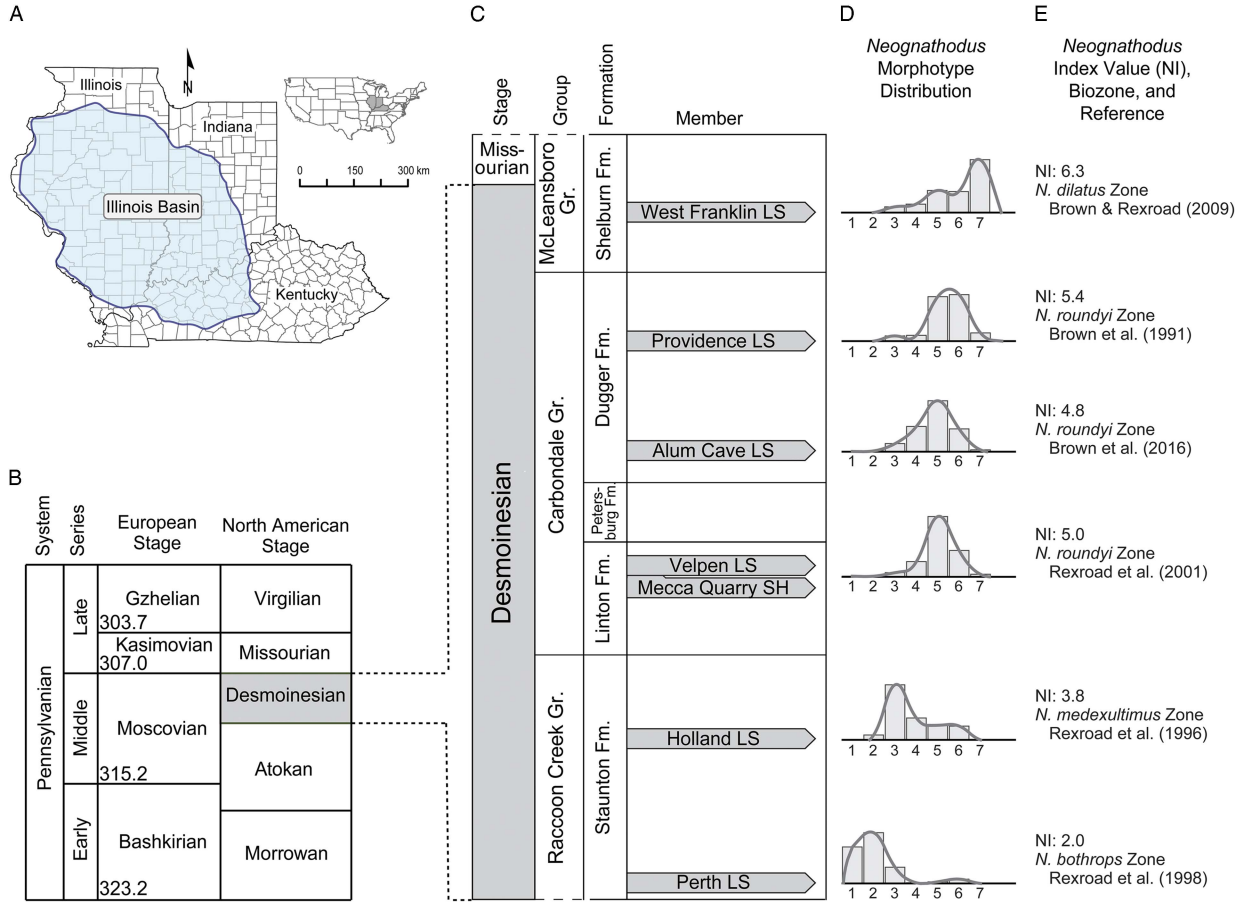

FIGURE 1. Summary of previous *Neognathodus* work from the Desmoinesian of the Illinois Basin. A, Extent of the Illinois Basin during the Desmoinesian (Tri-State Committee 2001). B, Chart of European and North American stages in the Pennsylvanian; adapted from Cohen et al. (2013). C, Stratigraphic nomenclature of the Desmoinesian (Middle–Late Pennsylvanian) in Indiana. Stratigraphic units examined in this study are highlighted in gray. Stratigraphy is adapted from Shaver et al. (1986), Tri-State Committee (2001), and Swezey (2009). Lithologic unit thicknesses are not to scale. Fm, formation; Gr., group; LS, limestone; and SH, shale. D, Histograms showing the distribution of *Neognathodus* morphotypes for each stratigraphic interval. Height of histogram bars are in percent, and all bars within a histogram total 100%. Morphotypes are numbered from oldest to youngest along the x-axis (1 = *N. bassleri*, 2 = *N. bothrops*, 3 = *N. medadultimus*, 4 = *medexultimus*, 5 = *N. roundyi*, 6 = *N. dilatus*, and 7 = *N. metanodosus*) The study that published each distribution is shown to the right in part V. E, Published *Neognathodus* Index (NI) value, named biozone for each interval, and references to published works for each unit. The NI is the weighted average of each morphotype distribution.

N. bothrops Merrill, 1972; *N. medadultimus* Merrill, 1972; *N. medexultimus* Merrill, 1972; *N. roundyi* (Gunnell 1931); *N. dilatus* (Stauffer and Plummer 1932); and *N. metanodosus* Merrill, 1975b? (2) How do statistical GM interpretations of morphologic change through the Desmoinesian compare with previous evolutionary interpretations? (3) Do GM results significantly affect previous biozonations of Illinois Basin units during the Desmoinesian? GM results will allow us to capture the full spectrum of shape variability within and among morphotype groups, provide a quantitative record of morphologic change through the extinction of the genus at the end of the Desmoinesian (Merrill 1975a; Merrill and Grayson 1989; Boardman et al. 1990), and supply the first quantitative evaluation of how GM-based biozonation compares with previous biozonation patterns. Due to the gradual transition in shape between morphotype groups (Merrill 1972, 1975a,b, 1999), we hypothesize GM groups will not be entirely congruent with previous morphotype groups. Previous evolutionary interpretations and biozones are based on the population-based NI; thus, we hypothesize that GM morphologic change through the Desmoinesian will support previous interpretations of evolution, and GM biozones will be similar in structure to published biozonations.

Certain considerations must be addressed regarding taxonomic boundaries and temporal shape variation. Our methods assume that an outline-based morphometric analysis will effectively characterize shape variability (Klapper and Foster 1993; Girard et al. 2004a, 2007) within and among morphotype groups and between *Neognathodus* populations through time. We also judge that morphologic changes of the *Neognathodus* P1 element are sufficiently documented through the Desmoinesian in the Illinois Basin (Brown et al. 1991, 2016; Rexroad et al. 1996, 1998, 2001; Brown and Rexroad 2009) to serve as a valid and established biostratigraphic proxy for comparing and statistically correlating with new GM patterns of *Neognathodus* morphologic change through time.

Quantitative characterizations of *Neognathodus* morphologies could offer valuable numeric evidence to document how conodont evolution was influenced by environmental change, especially during the global Desmoinesian glacial–interglacial iterations (Heckel 1991; Falcon-Lang et al. 2011). The Desmoinesian was dominated by an icehouse regime, as continental glaciations repeatedly occurred in southern Gondwana (Veevers and Powell 1987; Joachimski et al. 2006). These glacial repetitions altered climate conditions and sea levels in the tropical regions including the Illinois Basin (Poulsen et al. 2007; Tabor and Poulsen 2008). During glacial intervals, the tropical climate was drier and more seasonal, whereas during interglacial intervals, the tropical climate was more humid to subhumid (Falcon-Lang and DiMichele 2010). An intense glacial phase and regression followed by a warming and transgression likely occurred at the Desmoinesian–Missourian boundary (Falcon-Lang et al. 2011), and the extinction of multiple conodont groups at that boundary, including *Neognathodus* (Merrill 1975a; Merrill and Grayson 1989; Boardman et al. 1990), could have resulted from these major climatic changes (Falcon-Lang et al. 2011).

Materials and Methods

We photographed 390 specimens of *Neognathodus* P1 elements for GM analysis. Our project examined *Neognathodus* specimens published in six prior studies (Brown et al. 1991, 2016; Rexroad et al. 1996, 1998, 2001; Brown and Rexroad 2009). Specimens were spatially sampled from locations in eastern Illinois, northwestern Kentucky, and southwestern Indiana, and stratigraphically sampled from the following Desmoinesian units: Perth and Holland Limestone Members of the Staunton Formation, Mecca Quarry Shale and Velpen Limestone Members of the Linton Formation, Alum Cave and Providence Limestone Members of the Dugger Formation, and the West Franklin Limestone Member of the Shelburn Formation (Fig. 2). The Mecca Quarry Shale and Velpen Limestone Members were combined and sampled as one interval, because previous conodont sampling did not differentiate between the two members (Rexroad et al. 2001). For all units, the depositional environment is interpreted as a nearshore, deltaically influenced marine setting (Ferm et al. 1971;

https://doi.org/10.1017/pab.2018.28 Published online by Cambridge University Press

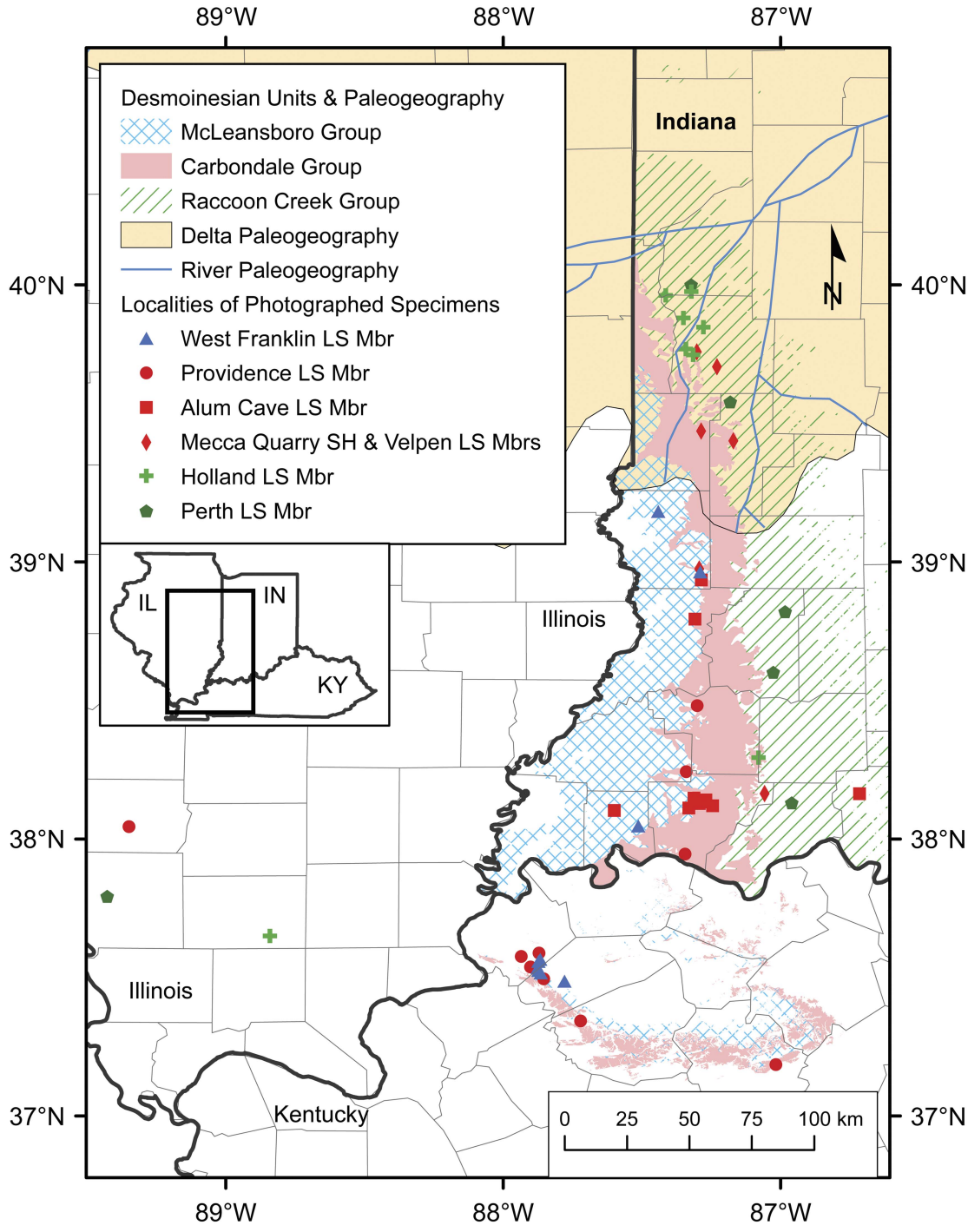

FIGURE 2. Map showing sampling localities and stratigraphic units of the 390 photographed specimens used in geometric morphometric (GM) analysis. Unit names are arranged in stratigraphic order, and dashed gray lines separate members of different stratigraphic groups. Detailed stratigraphic information is shown in Fig. 1. Outcrop data are sourced from Gray et al. (2010) for Indiana and from Noger et al. (1988) for Kentucky. Detailed, statewide outcrop maps were not available for Illinois. Generalized paleogeographic reconstructions of deltas and rivers during the Desmoinesian are superimposed and adapted from Jacobson (2000). LS, limestone; Mbr, member; SH, shale.

https://doi.org/10.1017/pab.2018.28 Published online by Cambridge University Press

Trask and Palmer 1986; Rexroad et al. 2001; Brown et al. 2016). Thus, any *Neognathodus* sample variation was likely not affected by changing paleoenvironments.

All specimens are housed in the Indiana University Paleontology Collection in the Department of Earth and Atmospheric Sciences at Indiana University, Bloomington, Indiana (catalog numbers in Supplementary Table 1). We selected specimens with a completely preserved and unbroken P1 element for photography. We photographed *Neognathodus* P1 elements with a digital microscope at 20× magnification at 1024 × 1660-pixel resolution. *Neognathodus* morphotypes are identified from an oral view of the P1 element, and we photographed and used the same view for GM analysis.

The 390 specimens comprised two different subsets, because we conducted two separate analyses. One subset was used to analyze morphotype group affinities, and we sampled specimens across stratigraphic boundaries to acquire 30 specimens per morphotype group. The other specimen subset was used to analyze *Neognathodus* morphologic change through the Desmoinesian, and we sampled 30 specimens per stratigraphic interval. Using two different specimen subsets allowed us to form a consistent sample size for each separate analysis, thereby avoiding the influence of sample size differences on results.

Sample Selection.—To test morphotype group affinities among *N. bassleri*, *N. bothrops*, *N. medadultimus*, *N. medexultimus*, *N. roundyi*, *N. dilatus*, and *N. metanodosus* we compiled data tables from previous studies (Brown et al. 1991, 2016; Rexroad et al. 1996, 1998, 2001; Brown and Rexroad 2009) and then counted the number of times each morphotype group occurred in every stratigraphic interval. For example, the *N. bassleri* morphotype group has 110 occurrences in the Perth Limestone Member, six occurrences in the Mecca Quarry Shale and Velpen Limestone Members, and four occurrences in the Alum Cave Limestone Member (Supplementary Table 2). We then totaled the number of occurrences for each morphotype group and used that sum to convert the raw occurrence data to percent occurrence data. For example, there were 120 *N. bassleri* occurrences across all units, which demonstrates that 92% of all *N. bassleri* specimens occur in the Perth Limestone Member (110/120 = 0.92), 1.5% occur in the Mecca Quarry and Velpen Limestone Members (6/120 = 0.015), and 1.0% occur in the Alum Cave Limestone Member (4/120 = 0.010). To replicate this stratigraphic morphotype distribution in our GM analysis, we selected 30 specimens from each of the seven morphotypes (total of 210 specimens), and then multiplied these percentages by 30 to determine the number of specimens to select and photograph from each stratigraphic interval (Table 1). For example, to acquire our 30-specimen sample for *N. bassleri*, we selected 27 *N. bassleri* specimens from the Perth Limestone (92% × 30 ≈ 27), two from the Mecca Quarry Shale and Velpen

TABLE 1. Table showing the stratigraphic distribution of *Neognathodus* specimens selected to test morphotype group affinities. Specimens were chosen between multiple stratigraphic boundaries. For example, to select the 30-specimen sample of *N. bassleri*, 27 *N. bassleri* specimens were chosen from the Perth Limestone Member, two were chosen from the Mecca Quarry Shale and Velpen Limestone Members, and one was chosen from the Alum Cave Limestone Member. LS, limestone, Mbr, member; SH, shale. The number of specimens selected from each unit is proportional to the total number of morphotype group occurrences in that unit.

		Neognathodus morphotype groups						
		N. bassleri	*N. bothrops*	*N. medadultimus*	*N. medexultimus*	*N. roundyi*	*N. dilatus*	*N. metanodosus*
Stratigraphic interval	West Franklin LS Mbr	0	0	2	2	2	3	20
	Providence LS Mbr	0	0	2	2	4	8	4
	Alum Cave LS Mbr	1	2	11	18	14	12	3
	Mecca Quarry SH and Velpen LS Mbrs	2	1	4	7	10	6	3
	Holland LS Mbr	0	1	6	1	0	1	0
	Perth LS Mbr	27	26	5	0	0	0	0
	Total no. of specimens	30	30	30	30	30	30	30

https://doi.org/10.1017/pab.2018.28 Published online by Cambridge University Press

Limestone (1.5% × 30 ≈ 2), and one from the Alum Cave Limestone (1.0% × 30 ≈ 1). We chose a sample size of 30 for each subset, because it provides statistically useful and significant results without requiring an excessively high amount of specimen and data processing.

To characterize *Neognathodus* morphologic change through the Desmoinesian in the Illinois Basin, we selected a representative, random sample of 30 *Neognathodus* specimens from each stratigraphic interval (total of 180 specimens). We used published occurrence data to select randomly, with replacement, 30 *Neognathodus* specimens from each stratigraphic interval (Supplementary Table 2) (Brown et al. 1991, 2016; Rexroad et al. 1996, 1998, 2001; Brown and Rexroad 2009). For example, one sampling run of the Perth Limestone Member selected 15 *N. bassleri* and 15 *N. bothrops* specimens. We repeated random sampling 5000 times and then recorded the number of specimens in each morphotype group for each run. After randomly choosing 30 specimens 5000 times, we averaged the results of all runs to produce a summarized mean list of 30 specimens from each of the six stratigraphic intervals (30 × 6 = 180 total specimens). This final mean list provided a representative random sample of 30 *Neognathodus* specimens to select and photograph from each stratigraphic interval (Table 2). For example, the final 30-specimen sample for the Perth Limestone Member consisted of 10 *N. bassleri* specimens, 14 *N. bothrops* specimens, 5 *N. medadultimus* specimens, and 1 *N. dilatus* specimen. We again chose a sample size of 30 for consistency with sample sizes in prior analyses.

Geometric Morphometric Data and Processing.—Our project followed standard landmark-based GM techniques that use landmarks (x, y points on an image) to quantitatively characterize shape (Bookstein 1991; Zelditch et al. 2004). The GM method requires that an equal number of landmarks be placed in the same order for each specimen's image. To meet this requirement, we rotated and vertically reflected photographs to a consistent orientation, with the outer parapet facing upward and the posterior tip of the P1 element facing to the right (e.g., see Fig. 3A). We removed the background of each image and a digital outline of 241 landmarks was placed to characterize the two-dimensional shape of each *Neognathodus* P1 element (Fig. 3A). Outline points were automatically placed at equal intervals using the freeware program tpsDig (Rohlf 2016a), which greatly reduced the likelihood of subjective landmark variability. We configured the coordinate data as a TPS file with tpsUtil (Rohlf 2016b) and then imported the TPS landmark file into Mathematica (Wolfram 2016) software using the freeware extension Geometric Morphometrics for Mathematica (Polly 2016).

Our configuration of 241 landmarks captured detailed P1 element shape variation while still using minimal computational power. The outline traced both the outer and

TABLE 2. Table showing the morphotype group counts of the specimens selected to analyze *Neognathodus* morphologic change through the Desmoinesian. Specimens were chosen from multiple morphotype groups within each stratigraphic interval. This selection of 30 specimens from each stratigraphic interval represents a random sample of the population of *Neognathodus* within that stratigraphic unit. For example, the 30-specimen random sample from the Perth Limestone Member consisted of 10 *N. bassleri* specimens, 14 *N. bothrops* specimens, and 1 *N. dilatus* specimen. LS, limestone, Mbr, member; SH, shale. The number of specimens to select from each morphotype group was determined using the average of 5000 random resampling runs.

		Neognathodus morphotype groups							
		N. bassleri	*N. bothrops*	*N. medadultimus*	*N. medexultimus*	*N. roundyi*	*N. dilatus*	*N. metanodosus*	Total no. of specimens
Stratigraphic interval	West Franklin LS Mbr	0	0	1	2	5	5	17	30
	Providence LS Mbr	0	0	1	2	12	13	2	30
	Alum Cave LS Mbr	0	'0	2	7	14	6	1	30
	Mecca Quarry SH and Velpen LS Mbrs	0	0	1	5	17	6	1	30
	Holland LS Mbr	0	1	15	6	4	4	0	30
	Perth LS Mbr	10	14	5	0	0	1	0	30

https://doi.org/10.1017/pab.2018.28 Published online by Cambridge University Press

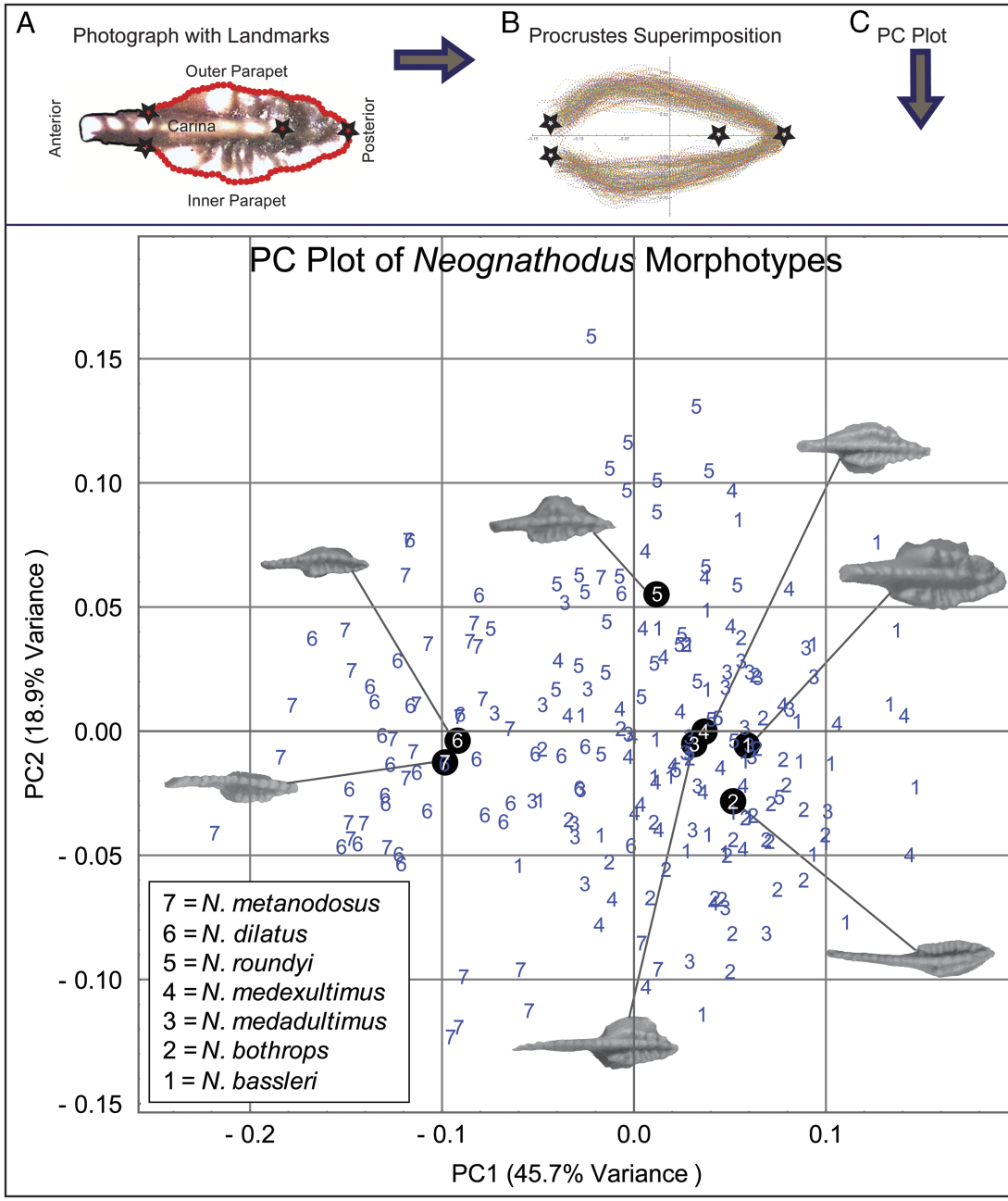

FIGURE 3. Diagram showing the methodology and results of morphotype group affinities. A, Photograph of a *N. bassleri* P1 element with a fully placed outline and annotated *Neognathodus* morphology. B, Thirty superimposed outlines of *N. bassleri*. Stars show similar locations in panels A and B. C, Scatter plot of PC 1 and PC 2 values for each specimen used to analyze morphotype group affinities. Every specimen is represented by a number corresponding to its morphotype group. The black dots correspond to the mean PC 1 and PC 2 coordinates of each morphotype group. Photographs of the P1 element for each morphotype group are also shown. PC signs are arbitrary, and the origin coordinates (0,0) represent the mean of PC 1 and PC 2, respectively. There is a gradual progression from the oldest morphotype (*N. bassleri* = 1) on the right to the youngest morphotype (*N. metanodosus* = 7) on the left.

https://doi.org/10.1017/pab.2018.28 Published online by Cambridge University Press

inner parapets of the P1 element, from the tip of the platform to the anterior section where both parapets meet with the carina. We placed one additional landmark at the posterior end of the carina to characterize carinal length (Fig. 3A). We did not outline the anterior edge of the carina, because it is usually broken and the morphology is indistinct and not significant among morphotypes (Merrill 1972, 1975b). We placed only one landmark on the posterior end of the carina, because (1) adding more points did not significantly affect later statistical results and (2) using only one point provided clear shape comparison of the P1 element outlines in subsequent visual analysis. We determined that 241 landmarks captured P1 shape variation better than an outline with a lower number of landmarks, because P1 shape changes were not as well visualized with fewer landmarks and statistical results were not stable below about 200 landmarks. Increasing the number of landmarks did not statistically change results and resulted in more computational resources and time for subsequent GM calculations.

Per common GM practices (Bookstein 1991; Zelditch et al. 2004), we superimposed the landmark coordinates from the images using Procrustes analysis and then calculated principal component (PC) scores. Procrustes analysis, described in detail by Rohlf and Slice (1990), first calculates the centroid of all landmarks, then centers that point on the origin of a Cartesian coordinate frame, scales the shape to a standard size, and finally rotates the shape to minimize distance variability (Fig. 3A). Following Procrustes superimposition, we performed principal components analysis (PCA) for each specimen outline to calculate PC scores. The GM data set is multidimensional; thus, PC scores act as convenient and consolidated shape variables to use in subsequent calculations and statistical tests. PC 1 shows the largest percent of shape variance, while each subsequent PC represents a progressively smaller amount of variance.

We created a scatter plot of PC 1 and PC 2 scores for both sets of specimens to visualize shape change in a PC morphospace. For the morphotype specimen set, we calculated the mean shape of each section in the PC scatter plot and displayed it as Procrustes coordinates in the form of thin plate splines (TPS). The TPS morphospace diagram shows average and extreme morphologies and illustrates which morphologic changes are described by the first two PC axes. The TPS calculations follow the methods of Hammer and Harper (2008), and we performed the mathematics using the function 'PrincipalComponentsOfShape' in Geometric Morphometrics for Mathematica (Polly 2016).

Quantitative Evaluations.—To evaluate shape similarity among both morphotype groups and stratigraphic units, we performed a multivariate analysis of variance (MANOVA) hypothesis test examining mean PC differences using the function 'ShapeMANOVA' in Geometric Morphometrics for Mathematica (Polly 2016), which performs a nonparametric randomization test for differences in group means. The null hypothesis of this test states there is no difference among the mean PC scores for each individual group of specimens, while the alternate hypothesis states there is a statistically significant difference among the mean PC scores for each individual group. This test is two tailed, uses all of the nonzero PC scores for each group, and compares each group to all other groups. We also performed nonparametric randomization to evaluate the significance of the difference in means among individual groups. This process randomized the groups and recalculated the difference 5000 times to assess significance. To account for the likely variability in *Neognathodus* P1 element shapes, we chose a significance level (alpha) of 0.10. This alpha also helps minimize type II statistical error (i.e., false-negative). Thus, a *p*-value greater than 0.10 would allow the null hypothesis, or no difference among mean shape, to be confidently rejected.

To evaluate how GM results might change morphotype diversity, we compared the number of GM groups with the number of morphotype groups at each sampling location. GM analysis coalesced morphotype groups, so the total number of distinct GM groups was less than the total number of morphotype groups. Therefore, we subtracted the number of GM groups from the number of morphotype groups at all previously published sampling

https://doi.org/10.1017/pab.2018.28 Published online by Cambridge University Press

localities of Brown et al. (1991, 2016), Rexroad et al. (1996, 1998, 2001), and Brown and Rexroad (2009). To summarize these results, we calculated the mean and median difference for each stratigraphic interval.

To assess morphologic changes through the Desmoinesian, we visually compared mean PC 1 values for each stratigraphic interval with published trends of the NI (Brown et al. 1991, 2016; Rexroad et al. 1996, 1998, 2001; Brown and Rexroad 2009). We calculated the mean PC 1 value for each stratigraphic interval and paired the mean PC 1 value with a stratigraphic depth to form a generalized time series showing average PC 1–based shape change through the Desmoinesian. We plotted the PC 1 time series with published NI trends of Brown et al. (2016) to visualize and compare the two patterns of changing *Neognathodus* morphology.

To quantitatively characterize *Neognathodus* P1 element shape change through the Desmoinesian, we conducted a maximum-likelihood evaluation of three evolutionary models following methods developed by Hunt (2006). The three models tested were an unbiased random walk (URW) with no directional component, a general random walk (GRW) that has a directional component, and stasis. This method fits the mean and variance of observed distribution of first differenced PC 1 values to their expectation under each of the three models (McKinney 1990). Following Hunt (2006), small-sample unbiased Akaike information criterion (Akaike 1974) and Akaike weights (Anderson et al. 2000) were used to select the model that best fits the observed PC 1 data. In terms of the evolutionary models, the mean determines the directionality, or tendency to change, and the variance determines the volatility of changes around the mean. The procedure requires an estimated age value, trait mean, and trait sampling error (i.e., variance) for each interval. We used age estimates for each stratigraphic interval from Tri-State Committee (2001) and Swezey (2009), calculated the mean and variance of PC 1 for each stratigraphic interval (i.e., no pooled variance), and performed the analysis using the function 'ThreeModelTest' in the Phylogenetics for Mathematica package (Polly 2018).

To quantitatively evaluate the relationship of GM morphologic patterns with the previous methods of interpreting evolution using NI values, we conducted a multivariate least-squares regression of shape using the function 'ShapeRegress' in Geometric Morphometrics for Mathematica (Polly 2016), which is a fully multivariate nonparametric randomization test for shape variables. The predictor value was the NI, and the response variable was each nonzero PC value of the mean shape for each stratigraphic interval. We determined the mean shape of all 30 specimens in each interval. All six mean outlines were Procrustes superimposed. We then calculated the PC scores of the averaged Procrustes-superimposed shape and regressed the PC scores onto the input, or NI, variable. To determine significance, we calculated the R-squared (R^2) values for the regression and the scores randomized with respect to the input variable, the NI, 10,000 times.

To assess how GM results affected previous biozonations, we determined GM-based biozones. First, we used the compiled data tables from prior studies (Brown et al. 1991, 2016; Rexroad et al. 1996, 1998, 2001; Brown and Rexroad 2009) to determine the percent abundance of every distinct GM group in each stratigraphic interval. If a GM group consisted of two previously separate morphotype groups, we combined the counts of both groups to find the total percent abundance for the GM group. We then assigned the GM biozone to the predominate GM group in each stratigraphic unit.

Results

Morphotype Group Affinities.—Calculations of all PC scores for the 210 *Neognathodus* specimens selected for testing morphotype group affinities show that PC 1 accounts for 45.7% of total shape variance, PC 2 accounts for 18.9%, and subsequent PCs progressively decrease in percent variance. MANOVA tests used all PCs and compared each morphotype with all other morphotypes, but for visual clarity, only PC 1 is shown in figures.

Plotting PC 1 and PC 2 values for each of the 210 *Neognathodus* specimens and the PC 1 and

https://doi.org/10.1017/pab.2018.28 Published online by Cambridge University Press

PC 2 mean of each morphotype group illustrates there is considerable shape overlap and similarity among morphotypes (Fig. 3C). Note that the signs of the PC axes are arbitrary and the x-axis and y-axis represent the mean of PC 1 and PC 2, respectively. The most noticeable point pattern follows PC 1, as the clusters for each morphotype group gradually progress from the oldest morphotype, *N. bassleri* (group 1), on the far right to the youngest morphotype, *N. metanodosus* (group 7), on the far left. Also, the morphotype pairs *N. medadultimus*/*N. medexultimus* (groups 3 and 4), and *N. dilatus*/*N. metanodosus* (groups 6 and 7) plot extremely close together, indicating each pair has highly similar average shapes.

The TPS morphospace diagram visually shows that PC 1 seems to capture the overall width of the P1 element, while PC 2 appears to capture the degree of parapet curvature (Fig. 4). First, it is important to note that PC 1 and PC 2 are statistically uncorrelated, thus the shape change across the diagram should not be interpreted diagonally. The vertical distance between P1 element landmarks increases from left to right along PC 1 for each individual row. The left TPS diagrams in the middle and bottom rows show the narrowest P1 elements. This region of the morphospace is primarily occupied by *N. dilatus* and *N. metanodosus*, the morphotypes with the narrowest P1 elements (Fig. 3C). The upper two diagrams in the

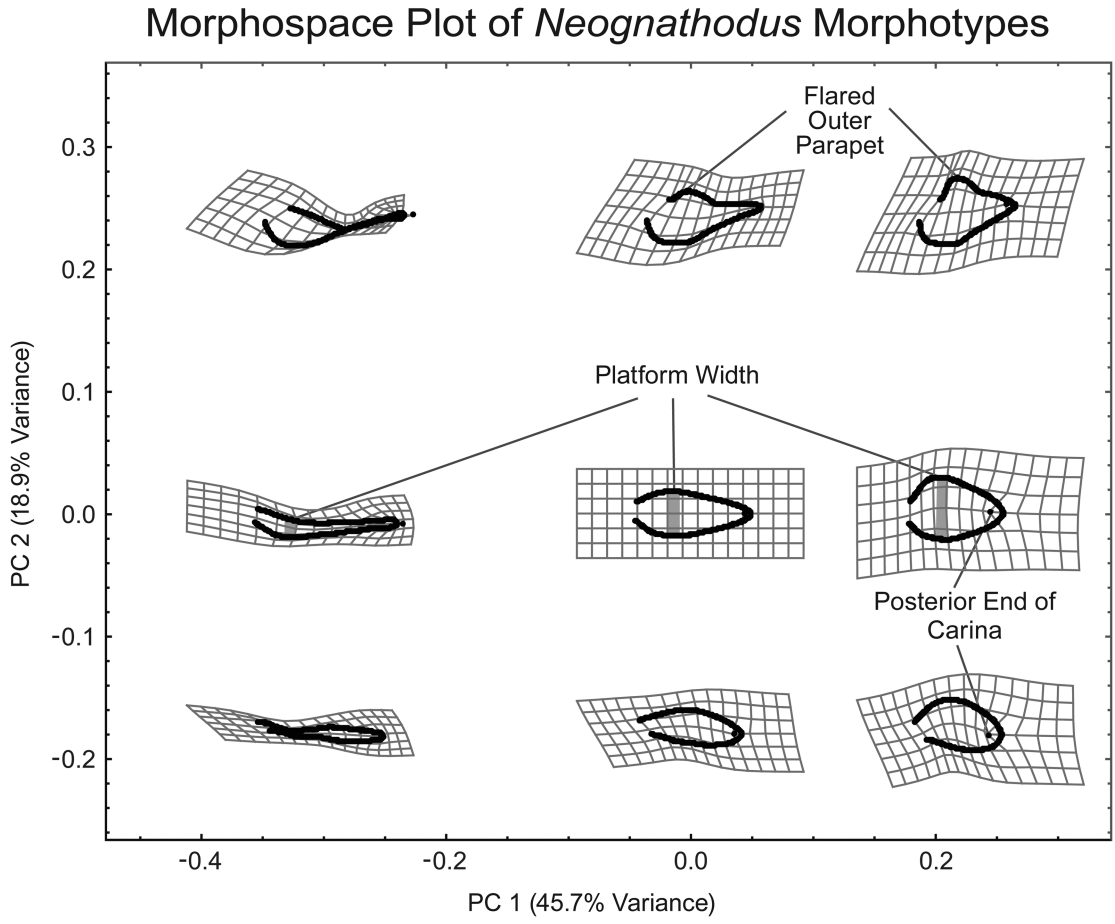

FIGURE 4. Morphospace diagram illustrating the average shape of *Neognathodus* P1 elements across PC 1 and PC 2 as thin plate splines. PC 1 and PC 2 are statistically uncorrelated, and shape change across the diagram should not be interpreted diagonally. This morphospace diagram spans a wider range of shape space then observed in Fig. 3 to better visualize and identify shape variation across PC 1 and PC 2. Note P1 element width increases from left to right along each row, and curvature of the parapets decreases from top to bottom along each column.

https://doi.org/10.1017/pab.2018.28 Published online by Cambridge University Press

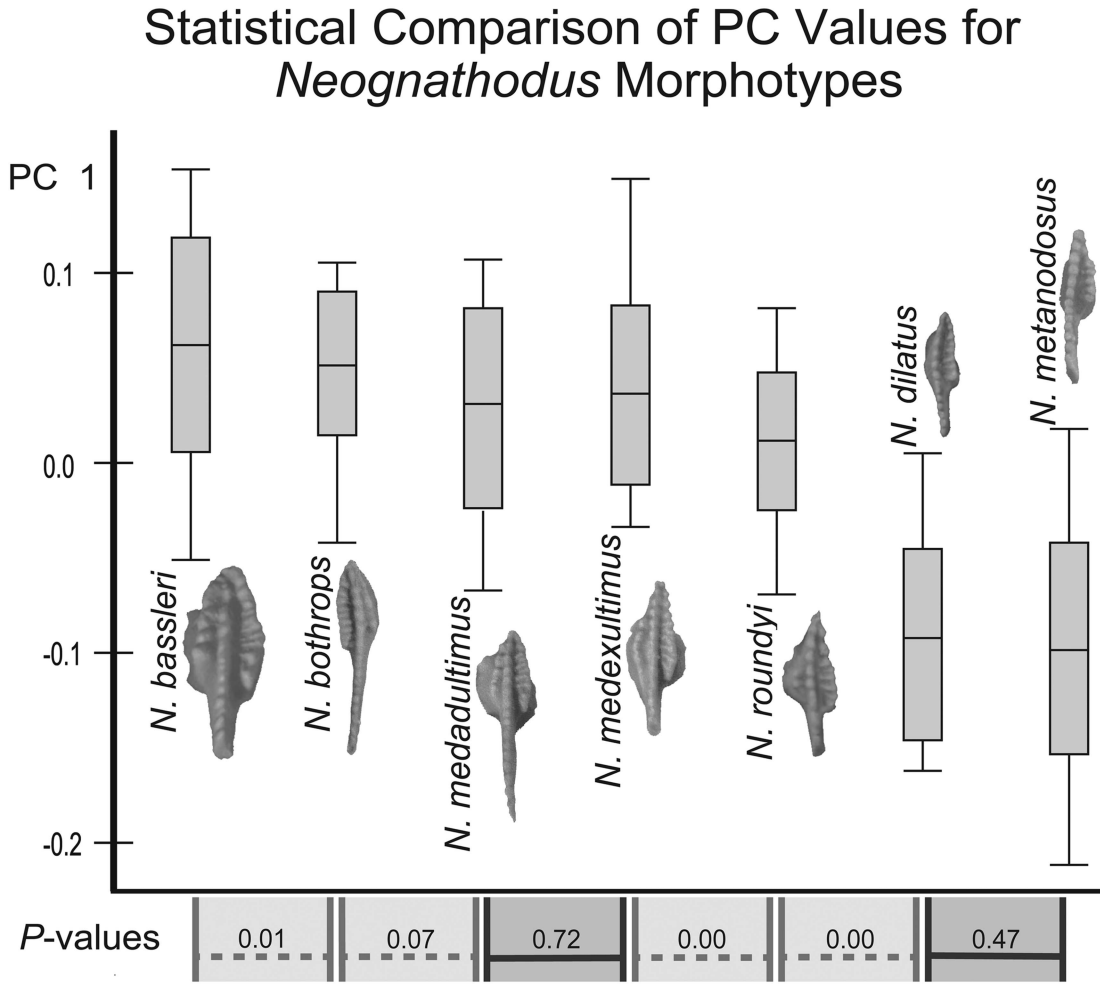

FIGURE 5. Diagram of PC 1 distributions for the 30-specimen sample of each analyzed *Neognathodus* morphotype group. Photographs of the P1 element for each morphotype are also shown. The *p*-values from MANOVA tests of all PC means are plotted on the x-axis. Dark gray intervals indicate morphotypes with statistically similar mean shapes (*p*-value > 0.10). MANOVA tests used all PCs and compared each morphotype with all other morphotypes. For visual simplicity, only PC 1 distributions of large *p*-values (*p*-value > 0.10) and of certain low *p*-values (*p*-value < 0.10) are shown. This analysis shows the morphotype pairs of *N. medadultimus* and *N. medexultimus* and *N. dilatus* and *N. metanodosus* do not exhibit a statistically significant difference in average P1 element shape.

middle and right columns are primarily composed of *N. roundyi* specimens that exhibit a similar distinct flare of the outer parapet (Fig. 4).

MANOVA tests of all PC means among *Neognathodus* morphotype groups provide *p*-values (Fig. 5) that support distinct groups among certain morphotypes and indistinct groups between others. Statistically distinct groups (i.e., *p*-values < 0.10 when compared with all other morphotype groups) include *N. bassleri*, *N. bothrops*, and *N. roundyi*. These statistically significant results, combined with the visually separate placement on morphospace plots, provide evidence that these groups are distinct in shape. Statistically indistinct groups (*p*-values > 0.10) include the morphotype pairs *N. medadultimus*/*N. medexultimus* and *N. dilatus*/*N. metanodosus*. The high *p*-values, in addition to the extremely close placement on morphospace plots, indicate these morphotype pairs are not distinct, and there is no meaningful, quantitative shape difference captured between *N. medadultimus* and *N. medexultimus*, and between *N. dilatus* and *N. metanodosus*.

https://doi.org/10.1017/pab.2018.28 Published online by Cambridge University Press

TABLE 3. Table summarizing, for each stratigraphic unit, how geometric morphometric (GM) group diversity results compare with previous diversity results based on morphotype group counts. For each stratigraphic interval, the median and mean value for the number of morphotype groups and the number of GM groups is shown, as is the median and mean difference between the two. Localities for each stratigraphic interval are plotted in Fig. 2. The stratigraphic units least affected by diversity loss are the Holland and Perth Limestone Members.

	No. of morphotype groups		No. of GM groups		Difference	
	Median	Mean	Median	Mean	Median	Mean
West Franklin LS Mbr	2.0	2.6	2.0	1.8	0.0	0.8
Providence LS Mbr	4.0	3.7	3.0	2.8	1.0	0.9
Alum Cave LS Mbr	4.0	3.5	3.0	2.7	1.0	0.8
Mecca Quarry SH and Velpen LS Mbrs	3.0	3.3	3.0	2.5	0.0	0.8
Holland LS Mbr	3.0	2.9	2.0	2.3	1.0	0.6
Perth LS Mbr	3.5	3.1	3.5	3.1	0.0	0.0

Coalescing these statistically similar morphotype pairs decreases morphotype diversity in many of the previously published Desmoinesian sampling localities of Brown et al. (1991, 2016), Rexroad et al. (1996, 1998, 2001), and Brown and Rexroad (2009) across Indiana, Kentucky, and Illinois (Table 3). The only member to show no diversity loss (mean difference of 0) is the Perth Limestone Member. This member only contained *N. medadultimus* and older morphotypes, which remained as distinct groups in the GM analysis. All other members show a diversity loss up to one or two morphotype groups at certain sampling localities.

Morphologic Change and Biozonation through the Desmoinesian.—Calculations of all PC scores for the 180 *Neognathodus* specimens selected for characterizing morphologic change through the Desmoinesian demonstrate that PC 1 accounts for 38.0% of total shape variance, PC 2 accounts for 24.9%, and subsequent PCs progressively decrease in percent variance. MANOVA tests used all PCs and compared each morphotype with all other morphotypes, but for visual clarity, only PC 1 is shown in figures.

Plotting PC 1 and PC 2 values for each of the 180 *Neognathodus* specimens illustrates there is considerable shape similarity between stratigraphic interval samples (Fig. 6). The most noticeable pattern follows PC 1 as the point clusters for each stratigraphic interval quickly progress from the oldest unit, Perth Limestone Member, on the right, to youngest unit, West Franklin Limestone Member, on the left. The means for the Mecca Quarry Shale/Velpen Limestone Members and the Alum Cave and Providence Limestone Members plot relatively close together, indicating all three units have similar average shapes.

MANOVA tests of all PC means between *Neognathodus* samples from each stratigraphic interval show *p*-values (Fig. 7C) that exhibit periods of both statistically distinct and similar mean shape through the Desmoinesian. There are statistically significant *p*-values (p-value < 0.10) from the Perth Limestone Member to the Holland Limestone Member and to the Mecca Quarry Shale/Velpen Limestone Members. These statistically significant results, combined with the visually separate placement on the PC plot, provide evidence that the mean shape for each successive interval is distinct. In contrast, statistically insignificant *p*-values (p-value > 0.10) are shown from the Mecca Quarry Shale/Velpen Limestone Members to the Alum Cave and Providence Limestone Members. The high *p*-values, as well as the extremely close placement on the PC plot, indicate that the mean shapes in these intervals are not distinct. Statistically significant *p*-values and separate PC means are again observed from the Providence Limestone Member to the West Franklin Limestone Member, indicating mean shape is distinct between the two.

A visual comparison of PC 1 averages and NI values for each stratigraphic interval shows a first-order similarity between both time series, and although certain differences are noticeable (Fig. 7D), additional statistical tests provide a strong correlation between the two (Fig. 8). The most apparent difference occurs

https://doi.org/10.1017/pab.2018.28 Published online by Cambridge University Press

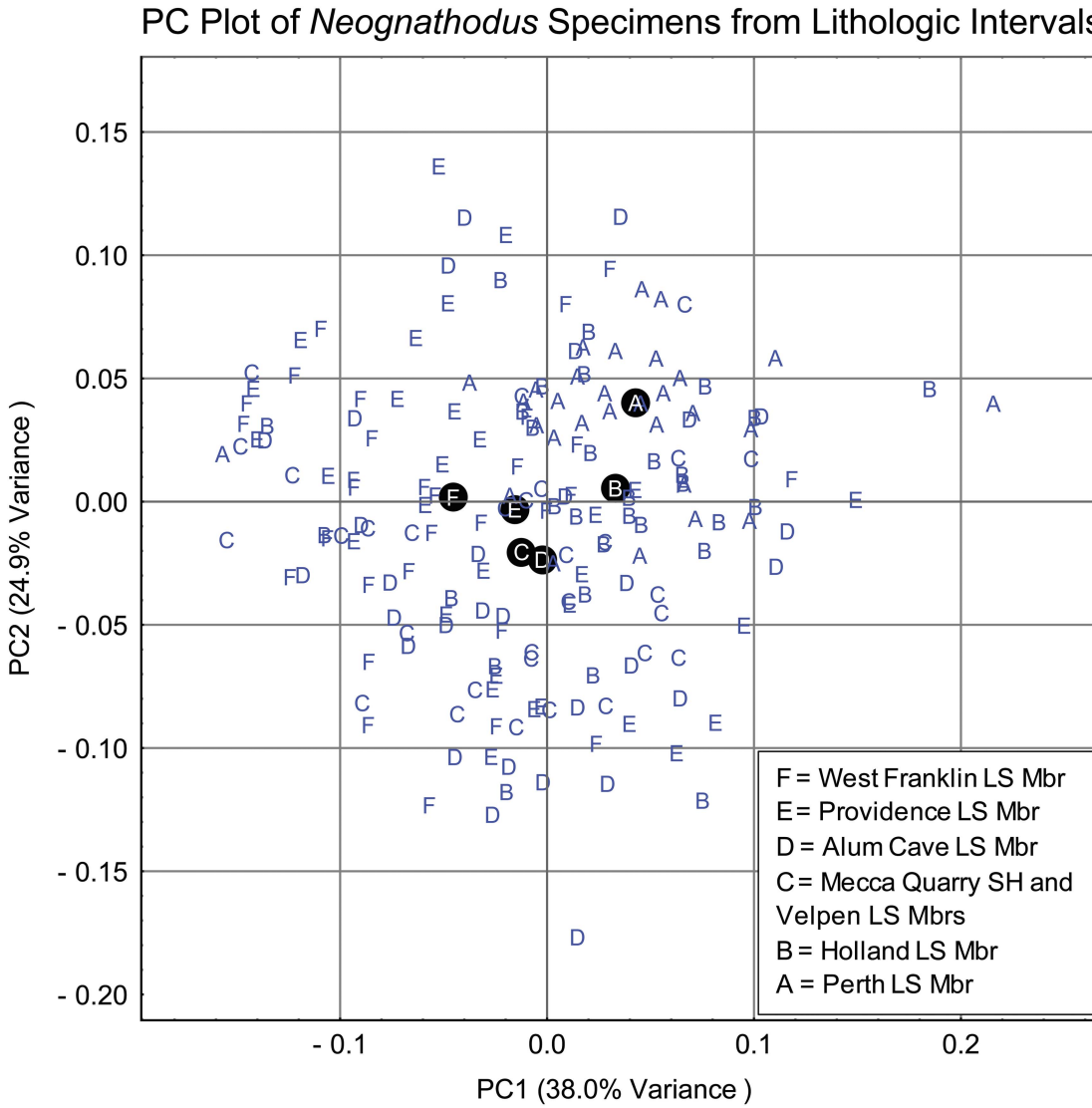

FIGURE 6. Scatter plot of PC 1 and PC 2 values for each specimen used to analyze *Neognathodus* morphologic change through time. Every specimen is represented by a letter corresponding to its stratigraphic interval. The black dots correspond to the mean PC 1 and PC 2 coordinates of the average shape of each stratigraphic interval sample. PC signs are arbitrary, and the origin coordinates (0,0) represent the mean of PC 1 and PC 2, respectively. There is a gradual progression from the oldest stratigraphic interval sample (Perth Limestone Member = A) on the right to the youngest sample (West Franklin Limestone Member = F) on the left. LS, limestone; Mbr, member; SH, shale.

where the NI value shows a large change from the Perth to the Holland Limestone Members, but the PC 1 mean exhibits relatively less change. Multi- and univariate regressions show primarily strong correlation strengths between PC means and NI values for each stratigraphic interval (Fig. 8). The multivariate regression of all nonzero PC means onto the NI resulted in an R^2 value of 0.67, meaning that 67% of the total shape variance in the PC means is predictable from the correlation to the NI. In contrast, the univariate regression of PC 1 means onto the NI increased the R^2 to 0.91.

The maximum-likelihood tests for evolutionary modes resulted in almost equally strong support for a URW with no directional component and a GRW with a directional component (Table 4). Akaike weights indicate that the model with the highest support is URW at 0.539, but GRW also has substantial

https://doi.org/10.1017/pab.2018.28 Published online by Cambridge University Press

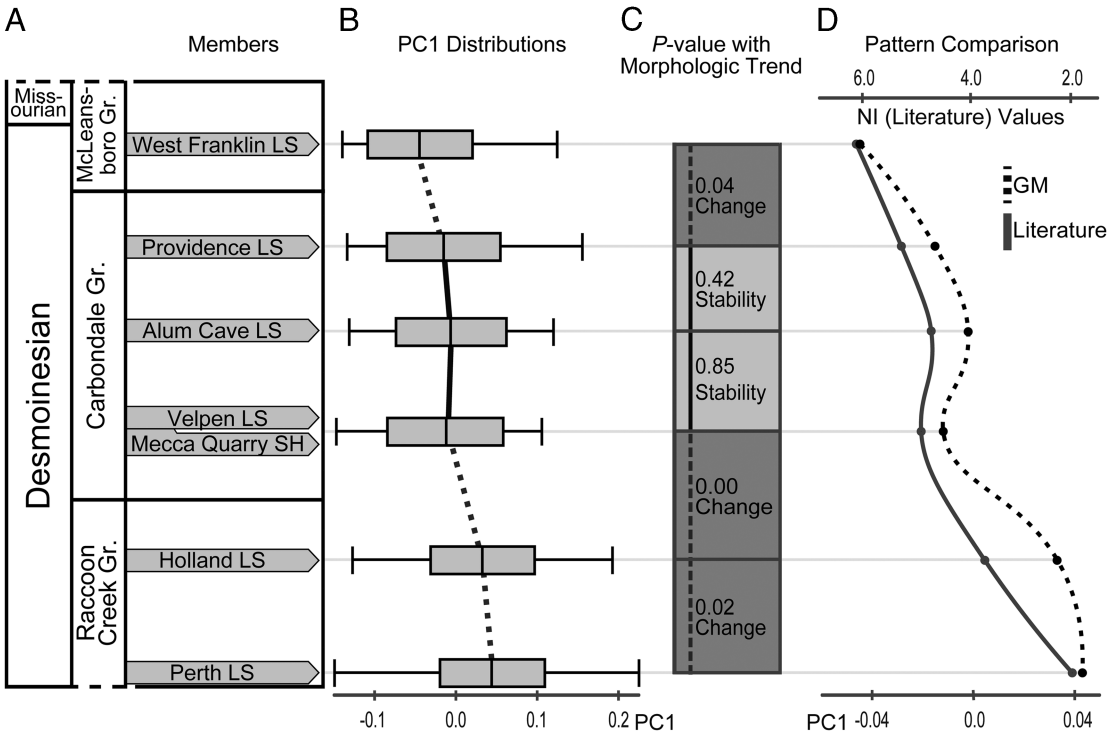

FIGURE 7. Diagram comparing geometric morphometric (GM) and published patterns of *Neognathodus* morphologic change through the Desmoinesian in the Illinois Basin. A, Summary chart showing the relative stratigraphic placement of each analyzed interval. B, Diagram of PC 1 distributions for the 30-specimen sample of each analyzed stratigraphic interval through the Desmoinesian. C, The *p*-values from MANOVA tests of all PC means are plotted along the y-axis. Dark gray intervals indicate stratigraphic intervals with statistically similar mean shapes (*p*-value > 0.10) and are interpreted as morphologic stability. MANOVA tests used all PCs and compared each stratigraphic interval with all intervals. For visual simplicity, only PC 1 distributions of large *p*-values (*p*-value > 0.10) and of certain low *p*-values (*p*-value < 0.10) are shown. D, Graph comparing the new GM interpretations to the published patterns of *Neognathodus* shape change, which are represented by *Neognathodus* Index (NI) values (Brown et al. 1991, 2016; Rexroad et al. 1996, 1998, 2001; Brown and Rexroad 2009). The dashed line labeled "GM" uses the bottom scale of "PC1," while the solid line labeled "Literature" uses the top scale of "NI (Literature) Values." Despite minor differences in magnitude, the overall trends (i.e., morphologic change and stability) are relatively similar. Gr., group; LS, limestone; SH, shale.

support at 0.405, while stasis has the least support at 0.055.

Determination of GM biozones resulted in the creation of four distinct biozonations through the Desmoinesian for all examined stratigraphic intervals (Fig. 9B). The GM biozones for the stratigraphic units are assigned as follows: Perth Limestone Member lies in the *N. bothrops* Zone; Holland Limestone Member resides in the *N. medadultimus* and *N. medexultimus* Zone; Mecca Quarry Shale, Velpen Limestone, Alum Cave Limestone, and Providence Limestone Member lie in the *N. roundyi* Zone; and the West Franklin Limestone Member resides in the *N. dilatus* and *N. metanodosus* Zone.

Discussion

Implications for Neognathodus Taxonomy.—Variability and transitional forms between *Neognathodus* morphotypes were recognized by Merrill (1972, 1975a,b, 1999), and our GM analysis alleviates the problem of documenting and classifying gradual morphologic transitions between morphotype groups. GM analysis does not place specimens into separate bins, and results illustrate and record the entire gradual spectrum of shape variability among morphotypes (Fig. 4). Morphotype groups transition along PC 1, indicating the shape traits used for morphotype group classification are best captured by PC 1 (Fig. 3C). Subsequent PCs are valuable for capturing additional

https://doi.org/10.1017/pab.2018.28 Published online by Cambridge University Press

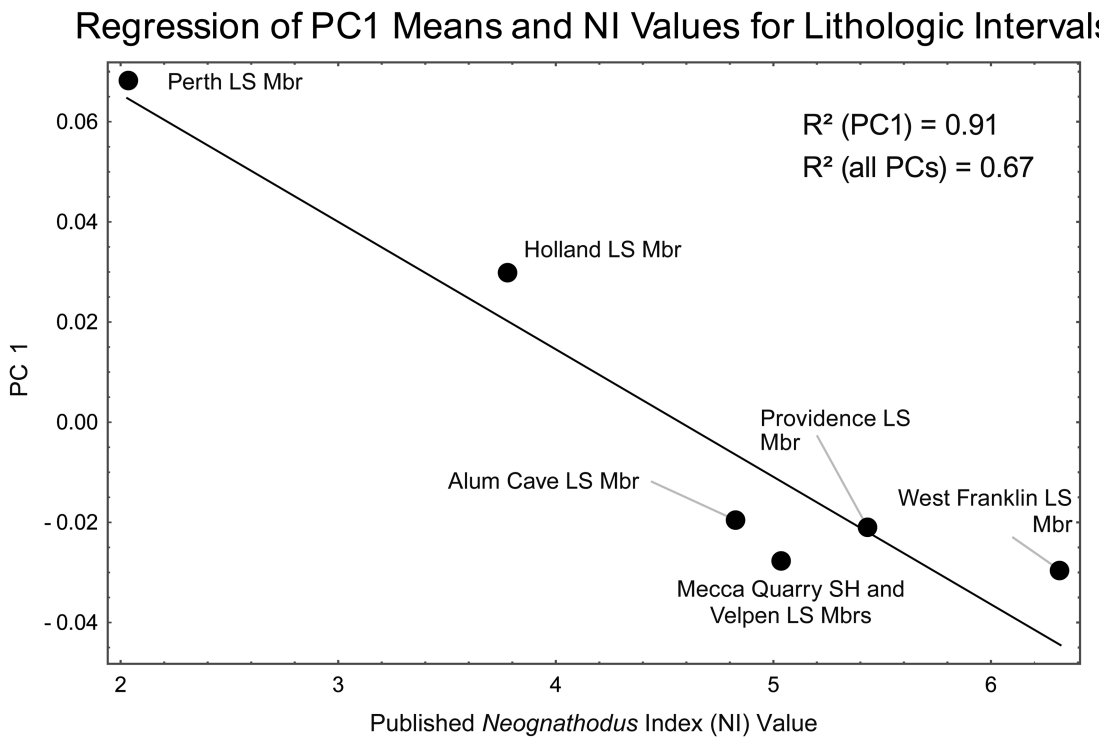

FIGURE 8. A univariate least-squares regression of shape for all mean PC 1 values onto all *Neognathodus* Index (NI) values. The NI values represent the previously published patterns of *Neognathodus* morphologic change through the Desmoinesian (Brown et al. 1991, 2016; Rexroad et al. 1996, 1998, 2001; Brown and Rexroad 2009). Regressing the NI onto only PC 1 provides an R^2 of 91%, while using all of the PCs decreases the R^2 to 67%. LS, limestone; Mbr, member; SH, shale.

TABLE 4. Table summarizing results of maximum-likelihood evolutionary model fitting for patterns of *Neognathodus* morphologic change through the Desmoinesian in the Illinois Basin. Thirty PC 1 values from each of the six stratigraphic intervals were used to assess evolutionary model support for three models, an unbiased random walk (URW) with no directional component, a general random walk (GRW) that has a directional component, and a stasis model (Stasis). Terminology and methods follow Hunt (2006). *K* is the number of parameters in each model; AIC_c is the small-sample, unbiased Akaike information criterion; σ_{step} is the estimated step variance for the URW and GRW models; μ_{step} and θ are the estimated step means for the GRW and Stasis models, respectively; ω is the estimated step variance for the Stasis model; and Akaike weights show model support. Variance was not combined across stratigraphic intervals due to significant variance differences. The σ_{step} parameter is rounded to zero but is actually just very small (<0.00000000001). URW (0.539) and GRW (0.405) models provide the strongest support (in bold), and Stasis (0.055) supplies the least support.

Model	*K*	Parameters	AIC_c	Akaike weights
URW	1	$\sigma_{step} = 0.000$	−17.038	**0.539**
GRW	2	$\mu_{step} = -0.033$, $\sigma_{step} = 0.000$	−16.468	**0.405**
Stasis	2	$\theta = -0.009$, $\omega = 0.001$	−12.487	0.055

aspects of shape variability, and all nonzero PCs should be used. For example, PC 2 differentiates *N. roundyi* more effectively than PC 1, because PC 2 captures the unique curvature of the outer parapet. Using all PCs provides full quantitative characterization of these gradual morphology shifts and allows for thorough and objective statistical testing of shape similarity.

Analysis of morphotype statistical tests (Fig. 5) and the morphotype PC plot (Fig. 3C) shows that GM groups are not entirely congruent with previous morphotype groups. This result supports our initial hypothesis of some

https://doi.org/10.1017/pab.2018.28 Published online by Cambridge University Press

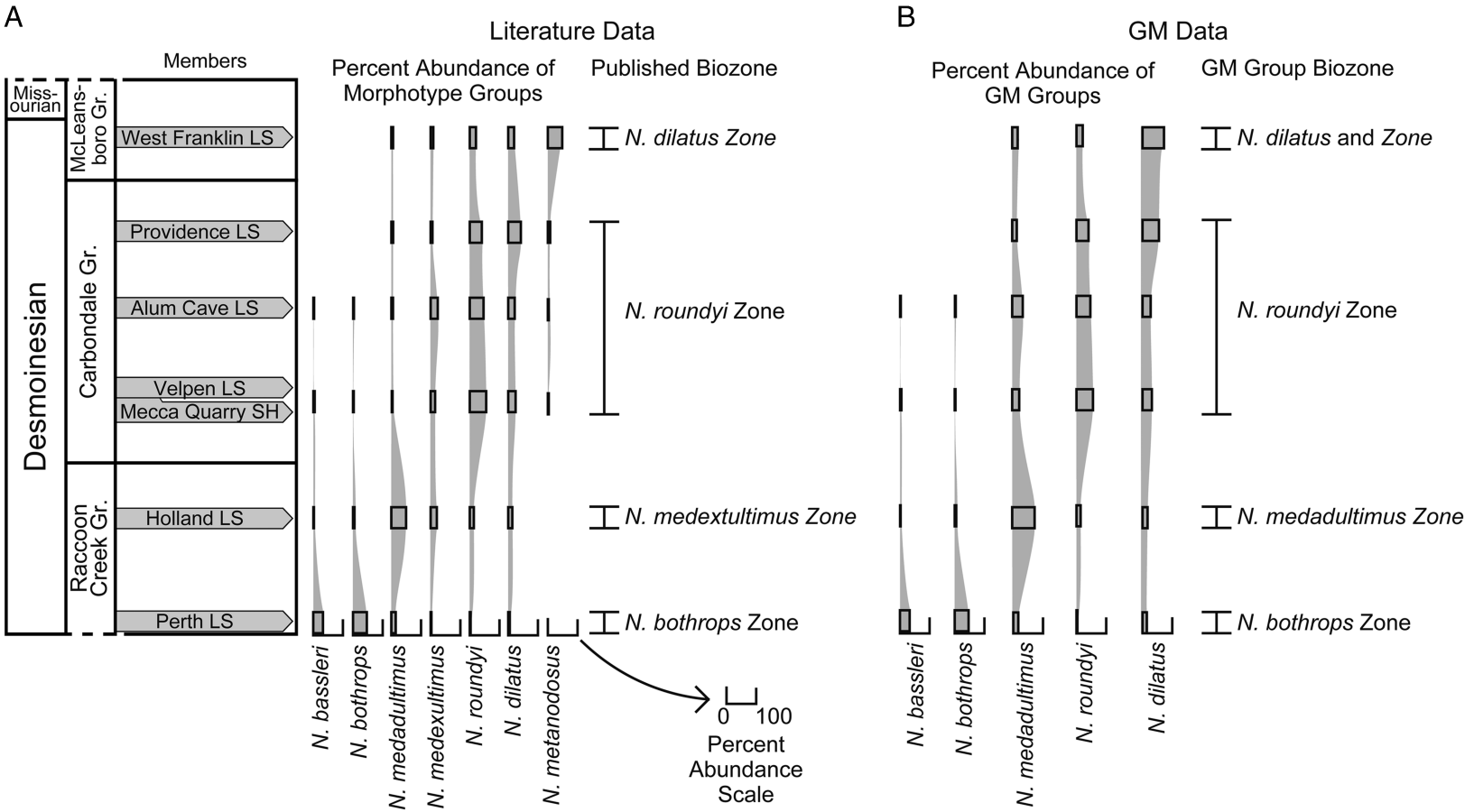

FIGURE 9. Comparison of published *Neognathodus* biozones with new geometric morphometric (GM) results. A, Percent abundance of each *Neognathodus* morphotype group through the Desmoinesian and named biozone for each stratigraphic interval. B, Percent abundance of each *Neognathodus* GM group and the resulting biozone name for each interval. Although the structures and names of the biozones are identical, the literature and GM biozonations were determined using significantly different methodologies. The biozones for the literature data were determined and named using the *Neognathodus* Index. In contrast, the GM biozones were determined with statistical tests of GM-based shape and named using the percent abundances of GM groups. The GM biozones (right side) use our synonymized morphotype pairs of *N. medadultimus*/*N. medexultimus* to *N. medadultimus* and *N. dilatus*/*N. metanodosus* to *N. dilatus*. Gr., group; LS, limestone; SH, shale.

dissimilarity among GM and morphotype groups. The statistically distinct GM groups align with and support previously established classifications of *N. bassleri* (Harris and Hollingsworth 1933), *N. bothrops* Merrill, 1972, and *N. roundyi* (Gunnell 1931). In contrast, the statistically indistinct pairs of GM groups are incongruent with and do not support literature designations of *N. medadultimus* Merrill, 1972/*N. medexultimus* Merrill, 1972 and *N. dilatus* (Stauffer and Plummer 1932)/*N. metanodosus* Merrill, 1975b. Coalescing indistinct morphotype groups decreases the number of unique groups (i.e., diversity) across most sampled localities (Table 3). Despite the apparent loss of any diversity, GM analysis still records the full spectrum of morphologic variability for all photographed specimens in the form of objective and quantitative PC distributions.

In both indistinct morphotype pairs, we judge that GM statistical results provide sufficient support to officially synonymize each morphotype pair. The key morphologic difference between *N. medadultimus* and *N. medexultimus* is that the outer posterior parapet of *N. medexultimus* is relatively shorter and shows slightly more anterior fusion with the carina (Merrill 1972). The primary difference between *N. dilatus* and *N. metanodosus* is that the inner posterior parapet in *N. metanodosus* is relatively shorter and exhibits slightly more anterior fusion with the carina (Merrill 1975b). Both the outer and inner posterior parapet length, shape, curvature, and position relative to the carina are captured effectively with our GM outlines, and the difference between the two pairs remains statistically indistinct. Therefore, we propose *N. medadultimus* and *N. medexultimus* be synonymized as *N. medadultimus*, and *N. dilatus* and *N. metanodosus* be synonymized as *N. dilatus* (synonymy naming prioritizes the first-named morphotype within each pair). Detailed systematics for the synonymy are presented in the Systematic Paleontology section of the Supplementary Material.

Regardless of the differences between the numbers of GM and morphotype groups, the observed overlap among morphotype specimens in PC morphospace (Fig. 3C) supports the published concept that *Neognathodus* species consist of populations of morphotypes (Merrill 1972, 1999). GM results exhibit a gradual progression from one morphotype group to the next (Fig. 3C). Even if morphotype groups were coalesced following GM group results, the concept of *Neognathodus* species as populations of morphotypes (Merrill 1972, 1999) would remain valid. Overall, the quantitative characterization of form variation, along with the objective verification of *Neognathodus* species concepts without reliance on species-level taxonomy, further validate the use of a landmarked-based GM approach to conodont morphometric research. Our work adds additional support to the research that shows outline-based morphometric analyses effectively characterize shape variability within a given conodont genus (Klapper and Foster 1993; Girard et al. 2004a, 2007). Given this validation, it is vital to evaluate how GM analysis describes *Neognathodus* shape change through time and how GM group results affect previous interpretations of evolution and biostratigraphic correlations.

Evaluating Neognathodus Evolution.—Previously, the NI was used to interpret *Neognathodus* evolution through the Desmoinesian in the Illinois Basin (Brown et al. 2016). As mentioned earlier, the NI is a weighted average of the morphotype population (i.e., the species) in a given stratigraphic unit (Brown and Rexroad 2009). Using the NI, Brown et al. (2016) summarized the following morphologic patterns: (1) change from the Perth to the Holland Limestone Members of the Staunton Formation and to the Mecca Quarry Shale and Velpen Limestone Members of the Linton Formation, (2) stability from the Mecca Quarry Shale and Velpen Limestone Members of the Linton Formation to the Alum Cave and Providence Limestone Members of the Dugger Formation, and (3) change from Providence Limestone Member of the Dugger Formation to the West Franklin Limestone Member of the Shelburn Formation (Fig. 7D).

Statistical tests and PC plots of *Neognathodus* samples from each examined stratigraphic interval support our hypothesis that GM patterns of *Neognathodus* P1 element shape change are generally similar to established patterns of morphologic change based on the NI. We

https://doi.org/10.1017/pab.2018.28 Published online by Cambridge University Press

interpret the following patterns through the Desmoinesian: (1) morphologic change occurs from the Perth to the Holland Limestone Members of the Staunton Formation and to the Mecca Quarry Shale and Velpen Limestone Members of the Linton Formation, (2) relative morphologic stability persists from the Mecca Quarry Shale and Velpen Limestone Members of the Linton Formation to the Alum Cave and Providence Limestone Members of the Dugger Formation, and (3) morphologic change again occurs from the Providence Limestone Member of the Dugger Formation to the West Franklin Limestone Member of the Shelburn Formation (Fig. 7). These morphologic patterns provide a fully quantitative characterization of *Neognathodus* shape change progressing into extinction of the genus at the end of the Desmoinesian (Merrill 1975a; Merrill and Grayson 1989; Boardman et al. 1990), and they also align with a summary of published NI trends (Brown et al. 2016). Furthermore, GM patterns of P1 element shape change through the Desmoinesian retained a strong statistical correlation with the NI (Fig. 8). These morphologic patterns should be considered with additional evidence from lithologic information, previous interpretations of the depositional environment, and results of maximum-likelihood tests of evolutionary modes.

Overall, patterns of *Neognathodus* P1 element morphology through the Desmoinesian appear to be relatively independent of the lithology, sampling location, and depositional setting. The regional paleoenvironment remained relatively consistent through the Desmoinesian in the Illinois Basin. During this time, the basin was located along tropical latitudes and likely maintained a tropical to humid subtropical climate that was subject to wet and dry seasons (Cecil 1990). The lithologies for each examined member consist primarily of discontinuous limestone and interbedded shale (Shaver et al. 1986), and the depositional setting is interpreted as a nearshore marine environment with deltaic influence (Ferm et al. 1971; Trask and Palmer 1986; Rexroad et al. 2001; Brown and Rexroad 2009; Brown et al. 2016). A specific example of the independence between morphologic pattern and lithologies is evident between the Perth and Holland Limestone Members. Both consist of gray, fossiliferous limestone and belong to the same formation (Shaver et al. 1986), but morphologic change is interpreted between the two units. In contrast, morphologic stability is interpreted between the clastic-rich Mecca Quarry Shale and Velpen Limestone Members of the Linton Formation and the non-clastic Alum Cave and Providence Limestone Members of the Dugger Formation. These examples indicate that temporal patterns of *Neognathodus* P1 element morphology were not likely driven by localized environmental factors and do not obviously represent ecophenotypic variation. Instead, we evoke morphologic evolution as the major driver affecting P1 element morphology through the Desmoinesian.

Maximum-likelihood tests of evolutionary modes indicate the most likely models of P1 element morphologic evolution are a URW or a GRW (Table 4). Hunt (2006) states that only an evolutionary mode with an Akaike weight greater than 0.90 should be treated confidently as the most likely model. As such, we recognize our results show equivocal support for both URW (0.539) and GRW (0.405) modes. By the standards set by Hunt (2006), the mean for GRW is relatively small ($\mu_{step} = -0.033$), indicating that if GRW was the true model, then the directionality of the steps was relatively small. We also interpret the relatively low Akaike weight of the stasis model (0.055) to be significantly smaller than the other mode weights, and we support that stasis is an unlikely model for *Neognathodus* PC 1 evolution.

An important consideration is that restricting the analysis to only PC 1 values can potentially bias results toward the GRW model, because PC 1 shows the axis of greatest variance and likely shows a directional pattern in multivariate space (Bookstein 2013). Our results show statistically similar PC 1 means between certain stratigraphic intervals, and this suggests a directional bias is not inherent with our PC 1 data. Furthermore, Jones (2009) performed the same model tests (Hunt 2006) with PC 1 data from conodont P1 elements and demonstrated GRW was not overly favored.

Overall, our work supplies the first statistical assessment of *Neognathodus* evolutionary

https://doi.org/10.1017/pab.2018.28 Published online by Cambridge University Press

models in the Desmoinesian. Previous interpretations of *Neognathodus* evolution through the Desmoinesian provided highly useful generalized patterns of morphologic change based on the NI (Brown et al. 2016), and our GM work builds on that foundation by providing statistically significant, maximum-likelihood test results that support URW and GRW modes. Hunt's (2006) methods to interpret modes of evolution with maximum likelihood are applied by many researchers (Novack-Gottshall 2008; Jones 2009; Piras et al. 2012; Van Bocxlaer and Hunt 2013), and our results contribute to this work of documenting evolutionary patterns of significant fossil taxa. In sum, using our GM results with Hunt's (2006) evolution tests provides a fully quantitative means of characterizing conodont morphology and evolutionary partners without a priori classification of morphotypes or assumption of evolutionary modes.

Assessing Biostratigraphic Utility.—*Neognathodus* biozones have been used to correlate strata in the Illinois Basin throughthe Desmoinesian, and the NI was used to determine the *Neognathodus* biozone of each stratigraphic interval examined in this study (Brown et al. 2016). The morphotype name closest to the NI value represents the biozone name (1 = *N. bassleri*, 2 = *N. bothrops*, 3 = *N. medadultimus*, 4 = *medexultimus*, 5 = *N. roundyi*, 6 = *N. dilatus*, and 7 = *N. metanodosus*). For example, the Perth Limestone Member has an NI of 2.0, thus the member resides in the *N. bothrops* biozone (Rexroad et al. 1998). Biozonations for the remaining units are as follows: the Holland Limestone Member belongs to the *N. medadultimus* Zone (Rexroad et al. 1996); the Mecca Quarry Shale, Velpen Limestone, Alum Cave Limestone, and Providence Limestone Members all fall in the *N. roundyi* Zone (Brown et al. 1991, 2016; Rexroad et al. 2001); and the West Franklin Limestone Member belongs to the *N. dilatus* Zone (Brown and Rexroad 2009) (Fig. 1C). In sum, previous, NI-based work shows these Illinois Basin units reside in four *Neognathodus* biozones.

Our GM-based biozonations support the previous structure of four separate biozones through the Desmoinesian in the Illinois Basin units (Fig. 9) and our hypothesis that GM analysis would yield four similar biozonations. GM results coalesced the morphotype group pairs of *N. medadultimus*/*N. medexultimus* and *N. dilatus*/*N. metanodosus* (Fig. 5), but the structure of four distinct biozones remains intact (Fig. 9). Also, our GM-based biozonations show that stratigraphic intervals with statistically indistinct shapes lie within the same biozone. For example, *N. roundyi* is the published biozone for the Mecca Quarry Shale and Velpen Limestone Members (Rexroad et al. 2001), the Alum Cave Limestone Member (Brown et al. 2016), and the Providence Limestone Member (Fig. 1) (Brown et al. 1991). GM results show all of these units are also statistically indistinct in mean shape (Fig. 7). In addition, the stratigraphic intervals with statistically distinct mean shapes each reside in a different biozones, with the Perth Limestone Member in the *N. bothrops* Zone (Rexroad et al. 1998), the Holland Limestone Member in the *N. medadultimus* Zone (Rexroad et al. 1996), and the West Franklin Limestone Member in the *N. dilatus* Zone (Brown and Rexroad 2009).

The identical biozone structure between previous NI work and our GM analysis illustrates that *Neognathodus*-based biostratigraphic correlations would not change between methods. Thus, previous *Neognathodus*-based correlations both within the Illinois Basin and around North America would remain intact. Examples within the Illinois Basin include the correlation of the Alum Cave Limestone Member in Indiana with the St David Limestone Member of the Carbondale Formation in Illinois (Brown et al. 2016) and the correlation of the West Franklin Limestone Member of Indiana to the Lonsdale Limestone Member of the Shelburn Formation in northwestern Illinois (Brown and Rexroad 2009). Additional examples across North America include correlating units from Ohio (Merrill 1972), Texas (Grayson et al. 1985), and New Mexico (Brown et al. 2013) to units within the Illinois Basin.

Our GM-based biozonations also provide the first direct evaluation of how morphometric results compare with previous biozonations. Prior studies have coalesced certain conodont species that were useful for

https://doi.org/10.1017/pab.2018.28 Published online by Cambridge University Press

biostratigraphy and zonation (Renaud and Girard 1999; Girard et al. 2004a, 2007; Roopnarine et al. 2004), but these studies have not evaluated how morphometric-based biozones can be compared with previous, qualitative-based biozonations. Our GM analysis shows that objective and statistically robust morphologic results can be used to construct biozonations without relying on previous morphotype-level taxonomy. The structural similarity between previous NI-based and GM-based biozonations showcases that determining GM-based biozones is neither redundant nor unwarranted, as this comparison validates the use of landmark-based GM work for constructing viable biozonations and for subsequent stratigraphic correlations.

Conclusions

Our study provides the first morphometric work on the conodont genus *Neognathodus*, supplies the first statistical analysis of *Neognathodus* evolution in the Desmoinesian, and provides a broad-scale methodology to quantitatively test morphotype designations, interpret statistically robust morphologic change through time, and construct valid biozones. GM analysis fully differentiates *N. bassleri*, *N. bothrops*, and *N. roundyi* from all other *Neognathodus* morphotype groups and supports previous morphotype designations (Gunnell 1931; Harris and Hollingsworth 1933; Merrill 1972). In contrast, there is no statistically significant difference between the species pairs of *N. medadultimus*/*N. medexultimus* and between *N. dilatus*/*N. metanodosus*, suggesting these GM group pairs are incongruent with and do not support established species designations (Stauffer and Plummer 1932; Merrill 1972, 1975b). As such, we synonymize these pairs to *N. medadultimus* and *N. dilatus*, respectively. Coalescing taxonomic boundaries does not adversely affect patterns of morphologic change or biozonation structure. GM analysis of morphology patterns through time still shows periods of morphologic change and stability through the Desmoinesian that support previously published patterns (Brown and Rexroad 2009; Brown et al. 2016). Maximum-likelihood statistical tests of evolutionary modes indicate the most probable models of P1 element morphologic evolution are a URW (i.e., a Brownian motion random walk) or a GRW (i.e., directional change). Finally, our GM-based biozonations corroborate the previous structure of four distinct biozones in the Illinois Basin units through the Desmoinesian.

Although this study location is limited to the Illinois Basin, our quantitative methodology can be broadly applied to other geologic settings and additional conodont genera. Similarly, our work contributes an example of how GM results can be used with Hunt's (2006) maximum-likelihood tests to fully quantify conodont morphology and evolutionary patterns without categorizing morphotypes or assuming a null evolutionary model a priori. Previous morphometric outline analyses conducted on other conodont genera, such as the Late Devonian genus *Palmatolepis*, also exhibit a spectrum of transitional forms between species (Klapper and Foster 1993; Girard et al. 2004b, 2007). Although separated by more than 50 million years, both *Palmatolepis* and *Neognathodus* show similar gradational species boundaries. This indicates that it is valid and useful to pursue a standardized morphometric methodology of photography, outlining, and statistical testing to describe shape variation among many different conodont genera. In addition, the genera *Idiognathodus* and *Streptognathodus* are also used for Middle Pennsylvanian correlation, and species in both genera exhibit gradual shape variation between species morphologies (Barrick and Boardman 1989; Heckel 1991; Lambert 1992; Barrick et al. 1996, 2004). Thus, the genera are prone to the same inherently subjective taxonomic debate that affects *Neognathodus* zonation. Our quantitative approach to characterizing the range and significance of shape variation within each genus would form objective groups of species and may ultimately provide a robust framework with biostratigraphic utility in which to develop data-driven hypotheses for this significant chordate group.

Supplementary Material

Data available from the Dryad Digital Repository: https://doi.org/10.5061/dryad.1fm52vv

https://doi.org/10.1017/pab.2018.28 Published online by Cambridge University Press

Acknowledgments

We would like to thank L. Brown, professor emeritus in the Department of Geology at Lake Superior State University, and P. Novack-Gottshall, assistant professor in the Department of Biological Sciences at Benedictine University, for providing thorough and valuable reviews that significantly enhanced the quality of this manuscript. This research was supported in part by the Galloway-Perry-Horowitz Fellowship of Indiana University.

Literature Cited

Akaike, H. 1974. A new look at the statistical model identification. IEEE Transactions on Automatic Control 19:716–723.

Aldridge, R. J., and M. A. Purnell. 1996. The conodont controversies. Trends in Ecology and Evolution 11:463–4668.

Allmon, W. D. 2013. Species, speciation and palaeontology up to the Modern Synthesis: persistent themes and unanswered questions. Palaeontology 56:1199–1223.

Anderson, D. R., K. P. Burnham, and W. L. Thompson. 2000. Null hypothesis testing: problems, prevalence, and an alternative. Journal of Wildlife Management 64:912–923.

Barrick, J. E., and D. R. Boardman, II. 1989. Stratigraphic distribution of morphotypes of *Idiognathodus* and *Streptognathodus* in Missourian-lower Virgilian strata, north-central Texas. Pp. 167–188 *in* D. R. Boardman II, J. E. Barrick, J. M. Cocke, and M. K. Nestall, eds. Middle and Late Pennsylvanian chronostratigraphic boundaries in north-central Texas: glacial-eustatic events, biostratigraphy, and paleoecology, a guidebook with contributed papers, Part II. Contributed papers. Texas Tech University, Lubbock, Tex.

Barrick, J. E., D. R. Boardman, II, and P. H. Heckel. 1996. Biostratigraphy across the Desmoinesian–Missourian boundary in North America Midcontinent, USA: -mplications for defining the Middle–Upper Pennsylvanian boundary. IUGS Subcommision on Carboniferous Stratigraphy 34:161–175.

Barrick, J. E., L. L. Lambert, P. H. Heckel, and D. R. Boardman, II. 2004. Pennsylvanian conodont zonation for Midcontinent North America. Revista Espanola de Micropaleontologia 36:231–250.

Boardman, D. R., II, P. H. Heckel, J. E. Barrick, M. K. Nestall, and R. A. Peppers. 1990. Middle–Upper Pennsylvanian chronostratigraphic boundary in the Midcontinent region of North America. Pp. 319–337 *in* P. L. Brenckle and W. L. Manger, eds. Intercontinental correlation and division of the Carboniferous System. Courier Forschungsinstitut Senckenberg, Frankfurt.

Bookstein, F. L. 1991. Morphometric tools for landmark data: geometry and biology. Cambridge University Press, New York.

——. 2013. Random walk as a null model for high-dimensional morphometrics of fossil series: geometrical considerations. Paleobiology 39:52–74.

Brown, L. M., and C. B. Rexroad. 2009. Conodont paleontology of the West Franklin Limestone Member of the Shelburn Formation (Pennsylvanian) in the southeastern part of the Illinois Basin. Indiana Geological Survey Special Report 68:34.

Brown, L. M., C. B. Rexroad, D. L. Eggert, and A. S. Horowitz. 1991. Conodont paleontology of the Providence Limestone Member of the Dugger Formation (Pennsylvanian, Desmoinesian) in the southern part of the Illinois Basin. Journal of Paleontology 65:945–957.

Brown, L. M., C. B. Rexroad, and A. N. Zimmerman. 2013. Conodont biostratigraphy of the Porvenir Formation (Pennsylvanian, Desmoinesian) in the southeastern Sangre de Cristo Mountains, New Mexico. Mountain Geologist 50:99–119.

——. 2016. Conodont biostratigraphy of the Alum Cave Limestone Member of the Dugger Formation (Pennsylvanian, Desmoinesian), southwestern Indiana. Indiana Geological Survey Occasional Paper 72:25.

Cecil, C. B. 1990. Paleoclimate controls on stratigraphic repetition of chemical and siliclastic rocks. Geology 18:533–536.

Cohen, K. M., S. C. Finney, P. L. Gibbard, and J. X. Fan. 2013. The ICS international chronostratigraphic chart. International Commission on Stratigraphy Episodes 36:199–204.

Donoghue, P. C., M. A. Purnell, and R. J. Aldridge. 1998. Conodont anatomy, chordate phylogeny and vertebrate classification. Lethaia 31:211–219.

Donoghue, P. C., I. J. Sansom, and J. P. Downs. 2006. Early evolution of vertebrate skeletal tissues and cellular interactions, and the canalizationof skeletal development. Journal of Experimental Zoology and Molecular Developmental Evolution 306:1–17.

Falcon-Lang, H. J., and W. A. DiMichele. 2010. What happened to the coal forests during the Pennsylvanian glacial phases? Palaios 25:611–617.

Falcon-Lang, H. J., P. H. Heckel, W. A. DiMichele, B. M. J. Blake, C. R. Easterday, C. F. Eble, S. Elrick, R. A. Gastaldo, S. F. Greb, R. L. Martino, W. J. Nelson, H. W. Pfefferkorn, T. L. Phillips, and S. J. Rosscoe. 2011. No major stratigraphic gap exists near the middle–upper Pennsylvanian (Desmoinesian–Missourian) boundary in North America. Palaios 26:125–139.

Ferm, J. C., J. C. Horne, J. P. Swinchatt, and P. W. Whaley. 1971. Carboniferous depositional environments in northeastern Kentucky. Geological Society of Kentucky, Lexington, Ky.

George, T. N. 1956. Biospecies, chronospecies, and morphospecies. Pp. 17–31 *in* P. C. Sylvester-Bradley, ed. The species concept in paleontology. Systematics Association, London.

Gingerich, P. D. 1985. Species in the fossil record: concepts, trends, and transitions. Paleobiology 11:27–41.

Girard, C., and S. Renaud. 2011. The species concept in a long-extinct fossil group, the conodonts. Comptes Rendus Palevol 10:107–115.

Girard, C., S. Renaud, and D. Korn. 2004a. Step-wise morphological trends in fluctuating environments: evidence in the Late Devonian conodont genus *Palmatolepis*. Geobios 37:404–415.

Girard, C., S. Renaud, and A. Serayet. 2004b. Morphological variation of *Palmatolepis* Devonian conodont: species versus genera. Comptes Rendus Palevol 3:1–8.

Girard, C., S. Renaud, and R. Feist. 2007. Morphometrics of the Late Devonian conodont genus *Palmatolepis*: phylogenetic, geographical and ecological contributions of a generic approach. Journal of Micropalaeontology 26:61–72.

Gray, H. H., C. H. Ault, S. J. Keller, and D. Harper. 2010. Bedrock geology of Indiana. Indiana Geological Survey, Bloomington, Ind.

Grayson, R. C., Jr., E. L. Trice, III, and E. H. Westergaard. 1985. Significance of some middle Atokan to early Missourian conodont faunas from the Llano Uplift and Colorado River Valley, Texas. Southwest Section American Association of Petroleum Geologists Transactions, pp. 117–131.

Gunnell, F. H. 1931. Conodonts from the Fort Scott limestone of Missouri. Journal of Paleontology 5:244–252.

Hammer, O., and D. A. Harper. 2008. Palaeontological data analysis. Wiley-Blackwell, Oxford.

Harris, R. W., and R. V. Hollingsworth. 1933. New Pennsylvanian conodonts from Oklahoma. American Journal of Science 25:193–204.

Heckel, P. H. 1991. Lost Branch Formation and revision of upper Desmoinesian stratigraphy along Midcontinent outcrop belt. Kansas Geological Survey Geology Series 4:67.

Hunt, G. 2006. Fitting and comparing models of phyletic evolution: random walks and beyond. Paleobiology 32:578–601.
Jacobson, R. J. 2000. Pennsylvanian rocks in Illinois. Illinois State Geological Survey, Champaign, Ill.
Joachimski, M. M., P. H. von Bitter, and W. Buggisch. 2006. Constraints on Pennsylvanian glacioeustatic sea-level changes using oxygen isotopes of conodont apatite. Geology 34:277–280.
Jones, D. 2009. Directional evolution in the conodont Pteriospathodus. Paleobiology 35:413–431.
Jones, D., and M. A. Purnell. 2007. A new semi-automatic morphometric protocol for conodonts and a preliminary taxonomic application. Pp. 239–259 *in* N. MacLeod, ed. Automated taxon identifications in systematics. CRC Press (for Systematics Association), London.
Klapper, G., and C. T. Foster. 1986. Quantification of outlines in Frasnian (Upper Devonian) platform conodonts. Canadian Journal of Earth Science 23:1214–1222.
——. 1993. Shape analysis of Frasnian species of the Devonian condont genus *Palmatolepis*. Journal of Paleontology Memoir 32:1–35.
Lambert, L. L. 1992. Atokan and basal Desmoinesian conodonts from central Iowa, reference area for the Desmoinesian Stage. Oklahoma Geological Survey Circular 94:111–123.
Mayr, E. 1957. Species concepts and definitions. Pp. 1–22 *in* E. Mayr, ed. The species problem. American Association for the Advancement of Science, Washington, D.C.
——. 1996. What is a species, and what is not? Philosophy of Science 63:262–277.
McKinney, M. L. 1990. Classifying and analyzing evolutionary trends. Pp. 28–58 *in* K. J. McNamara, ed. Evolutionary trends. University of Arizona Press, Tucson, Ariz.
Merrill, G. K. 1972. Taxonomy, phylogeny, and biostratigraphy of *Neognathodus* in Appalachian Pennsylvanian rocks. Journal of Paleontology 46:817–829.
——. 1975a. Pennsylvanian conodont biostratigraphy and paleoecology of northwestern Illinois. Microform Publication 3: 100–130.
——. 1975b. Pennsylvanian conodonts of northwestern Illinois—summary and new systematics. Geology 3:721–722.
——. 1999. *Neognathodus* and the species concept in paleontology. Pp. 465–473 *in* E. Serpagli and C. Corradini, eds. Studies on conodonts. Bollettino della Societa Paleontologica Italiana 37:465–473.
Merrill, G. K., and R. C. Grayson, Jr. 1989. Conodont paleoecology of the type East Mountain Shale, north-central Texas. Pp. 147–154 *in* D. R. Boardman II, J. E. Barrick, J. M. Cocke, and M. K. Nestall, eds. Middle and Late Pennsylvanian chronostratigraphic boundaries in north-central Texas: glacial-eustatic events, biostratigraphy, and paleoecology, a guidebook with contributed papers, Part II. Contributed papers. Texas Tech University, Lubbock, Tex.
Murphy, M. A., and M. K. Cebecioglu. 1987. Morphometric study of the genus *Ancyrodelloides* (Lower Devonian, Conodonts), central Nevada. Journal of Paleontology 61:583–594.
Noger, M. C., R. C. McDowell, G. J. Grabowski, and S. L. Moore. 1988. Geologic map of Kentucky. Kentucky Geological Survey, Lexington, Ky.
Novack-Gottshall, P. M. 2008. Ecosystem-wide body-size trends in Cambrian–Devonian marine invertebrate lineages. Paleobiology 34:210–228.
Pander, C. H. 1865. Monographic der fossilen Fische des Silurischen Systems der Russisch-Baltischen Gouvernments. Saint Peterburg Académie des Sciences 1:91.
Piras, P., G. Sansalone, F. Marcolini, C. Tuveri, M. Arca, and T. Kotsakis. 2012. Evolutionary trends and stasis in molar morphology of Rhagapodemus–Rhagamys lineage in the Pleistocene of Sardinia. Rivista Italiana di Paleontologia e Stratigrafia 118:535–543.
Polly, P. D. 2016. Geometric morphometrics for Mathematica® package, Version 12.0. Indiana University, Bloomington, Ind.
——. 2018. Phylogenetics for Mathematica® package, Version 5.0. Indiana University, Bloomington, Ind.
Poulsen, C. J., D. Pollard, I. P. Montanez, and D. Rowley. 2007. Late Paleozoic tropical climate response to Gondwanan deglaciation. Geology 35:771–774.
Purnell, M. A. 1995. Microwear on conodont elements and macrophagy in the first vertebrates. Nature 374:788–800.
Renaud, S., and C. Girard. 1999. Strategies of survival during extreme environmental perturbations: evolution of conodonts in response to the Kellwasser crisis (Upper Devonian). Palaeogeography Palaeoclimatology Palaeoecology 146:19–32.
Rexroad, C. B., L. M. Brown, and S. L. Weinrick. 1996. *Idiognathodus* and the conodont biostratigraphy of the Holland Limestone Member, Staunton Formation (Pennsylvanian, Desmoinesian) from the Illinois Basin, U.S.A. Institute of Paleobiology, Polish Academy of Sciences: Sixth European Conodont Symposium (ECOS VI). Warsaw, Poland.
Rexroad, C. B., L. M. Brown, J. Devera, and R. Suman. 1998. Conodont biostratigraphy and paleoecology of the Perth Limestone Member, Staunton Formation (Pennsylvanian) of the Illinois Basin, USA. Palaeontologia Polonica 58:247–259.
Rexroad, C. B., J. A. Wade, G. K. Merrill, L. M. Brown, and P. Pagett. 2001. Conodont biostratigraphy and depositional environments of the Mecca Quarry Shale Member and the Velpen Limestone Member of the Linton Formation (Pennsylvanian, Desmoinesian) in the eastern part of the Illinois Basin, USA. Indiana Geological Survey Special Report 63:19.
Rohlf, F. J. 2016a. tpsDig, Version 2.22. Stony Brook University, Stony Brook, N.Y.
——. 2016b. tpsUtil, Version 1.67. Stony Brook University, Stony Brook, N.Y.
Rohlf, F. J., and D. Slice. 1990. Extensions of the Procrustes method for the optimal superimposition of landmarks. Systematic Biology 39:40–59.
Roopnarine, P. D., M. A. Murphy, and N. Buening. 2004. Microevolutionary dynamics of the Early Devonian conodont Wurmiella from the Great Basin of Nevada. Palaeontologia Electronica 8.2.31A.
Shaver, R. H., C. H. Ault, A. M. Burger, D. D. Carr, J. B. Droste, D. L. Eggert, H. H. Gray, D. Harper, N. R. Hasenmueller, W. A. Hasenmueller, A. S. Horowitz, H. C. Hutchison, B. D. Keith, S. J. Keller, J. B. Patton, C. B. Rexroad, and C. E. Weir. 1986. Compendium of Paleozoic Rock-Unit Stratigraphy in Indiana—A Revision. Indiana Geological Survey, Bloomington, Ind.
Sloan, T. R. 2003. Results of a new outline-based method for the differentiation of conodont taxa. Pp. 389–404 *in* R. Mawson and J. A. Taylor, eds. Second Australian Conodont Symposium (AUSCOS II). Courier Forschunginstitut Senckenberg, Orange, Australia.
Stauffer, C. R., and H. J. Plummer. 1932. Texas Pennsylvanian conodonts and their stratigraphic relations. University of Texas Bulletin 3201:13–50.
Sweet, W. C. 1988. The Conodonta: morphology, taxonomy, paleoecology and evolutionary history of a long-extinct animal phylum. Oxford Monographs on Geology and Geophysics 10:1–211.
Sweet, W. C., and P. C. Donoghue. 2001. Conodonts: past present, future. Journal of Paleontology 75:1174–1184.
Swezey, C. S. 2009. Regional stratigraphy and petroleum systems of the Illinois basin, U.S.A. USGS Scientific Investigations Map 3068. U.S. Geological Survey, Denver, Colo.
Tabor, N. J., and C. J. Poulsen. 2008. Palaeoclimate across the Late Pennsylvanian–Early Permian tropical palaeolatitudes: a review

of climate indicators, their distribution, and relation to palaeophysiographic climate factors. Palaeogeography, Palaeoclimatology, Palaeoecology 268:293–310.

Trask, C. B., and J. E. Palmer. 1986. Structural and depositional history of the Pennsylvanian System in the Illinois Basin. Pp. 63–78 *in* P. C. Lyons and C. L. Rice, eds. Paleoenvironmental and tectonic controls in coal-forming basins in the United States. Geological Society of America Special Paper 210.

Tri-State Committee on Correlation of the Pennsylvanian System Rock Units in the Illinois Basin. 2001. Toward a more uniform stratigraphic nomenclature for rock units (formations and groups) of the Pennsylvanian System in the Illinois Basin. Illinois Basin Consortium Illinois Basin Study 5. Illinois State Geological Survey, Indiana Geological Survey, Kentucky Geological Survey.

Van Bocxlaer, B., and G. Hunt. 2013. Morphological stasis in an ongoing gastropod radiation from Lake Malawi. Proceedings of the National Academy of Sciences USA 110:13892–13897.

Veevers, J. J., and C. M. Powell. 1987. Late Paleozoic glacial episodes in Gondwanaland reflected in transgressive–regressive depositional sequences in Euramerica. Geological Society of America Bulletin 98:475–487.

Vogt, L., T. Bartolomaeus, and G. Giribet. 2009. The linguistic problem of morphology: structure versus homology and the standardization of morphological data. Cladistics 26:301–325.

Wolfram. 2016. Mathematica®, Version 10.3. Wolfram Research, Champaign, Ill.

Zelditch, M. L., D. L. Swiderski, H. D. Sheets, and W. L. Fink. 2004. Geometric morphometrics for biologists: a primer. Elsevier Academic, San Diego, Calif.

https://doi.org/10.1017/pab.2018.28 Published online by Cambridge University Press